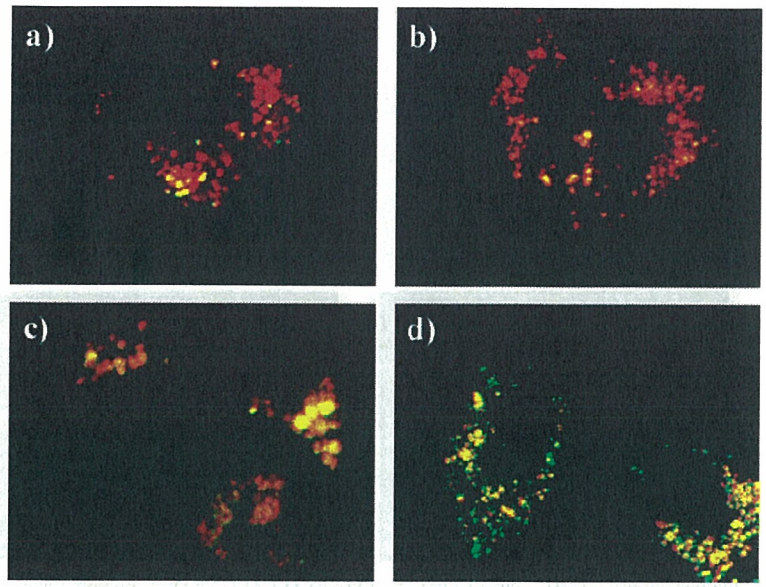

Figure 11. Confocal fluorescent microscope images of the HuH-7 cells in the presence of Lysotracker Red DND-99 and polyplex micelles prepared at N/P = 3 with FITC-labeled pDNA. (a) Lac-PEG-PAMA/pDNA polyplex micelles (incubation time: 30 min), (b) Lac-PEG-PAMA/pDNA polyplex micelles (incubation time: 120 min), (c) Lac-PEG-PSAO-PAMA/pDNA polyplex micelles, (incubation time: 30 min), (d) Lac-PEG-PSAO-PAMA/pDNA polyplex micelles (incubation time: 120 min). These images are the typical image of triplicate experiments.

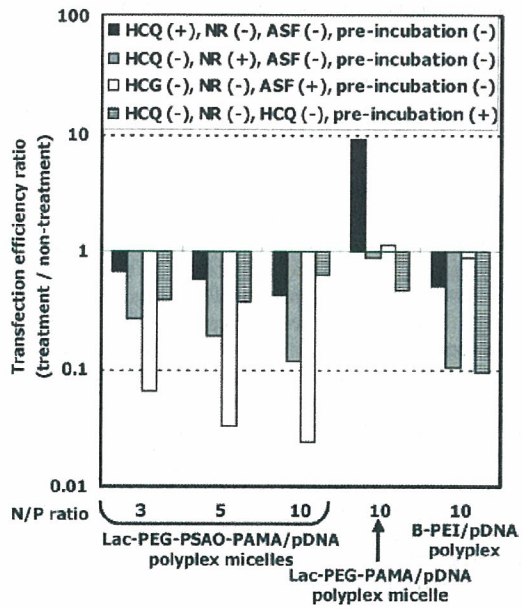

Figure 12. Effect of the HCQ (100 μM), NR (5 μM), ASF (4 mg/mL), and 20% serum preincubation on the transfection efficiency to HuH-7 cells of the Lac-PEG-PSAO-PAMA/pDNA polyplex micelle, Lac-PEG-PAMA/pDNA polyplex micelle, and B-PEI/pDNA polyplex as a function of N/P ratios at a fixed pDNA amount. Transfection efficiency ratio is described as [value of RLU/mg of protein treated with additive (HCQ, NR, and ASF)]/[value of RLU/mg of protein in Figure 11]. The plotted data are the average of triplicate experiments ± SD.

endosomal acidification, and ASF as an inhibitor of the ASGP-mediated endocytosis. As shown in Figure 12, HCQ treatment (100 μM) had no contribution in increasing the transfection efficiency for the Lac-PEG-PSAO-PAMA/pDNA polyplex micelles and the B-PEI/pDNA polyplex compared with the Lac-PEG-PAMA/pDNA polyplex micelle (about 1 order of magnitude increase in transfection efficiency), whereas it showed an appreciable decrease in the transfection efficiency in the presence of NR (5 μM) for the Lac-PEG-PSAO-PAMA/pDNA polyplex micelles and the B-PEI/pDNA polyplex. This is in line with the assumption that the Lac-PEG-PSAO-PAMA/pDNA polyplex micelles may be equipped with an endosome escaping function due to the unprotonated pH-responsive PSAO segment in the polyplex micelles.

A significant decrease in the transfection efficiency of the Lac-PEG-PSAO-PAMA/pDNA polyplex micelles was observed in the presence of ASF, consistent with the results of cellular uptake, as shown in Figure 9. Alternatively, no effect of ASF was observed even for the Lac-PEG-PAMA/pDNA polyplex micelle, suggesting that the endosomal escape may be the most critical barrier to intracellular gene delivery by Lac-PEG-PAMA/pDNA polyplex micelle. Thus, it may be reasonable to conclude that an appreciable fraction of the Lac-PEG-PSAO-PAMA/pDNA polyplex micelles is taken up into HuH-7 cells through the ASGP receptor-mediated endocytosis process mediated by the cluster of the large number of lactose moieties on the surface of the polyplex micelles, followed by the effective disruption of the endosome by the buffer effect of the unprotonated pH-responsive PSAO segment in the polyplex micelles.

It is well-known that components of the serum may interact with the polyplex to induce its structure change, resulting in decreasing transfection efficiency. Thus, we examined the effect of the 20% serum preincubation for 6 h on the transfection efficiency of Lac-PEG-PSAO-PAMA/pDNA, Lac-PEG-PAMA/pDNA polyplex micelles, and B-PEI/pDNA polyplexes. As shown in Figure 12, 1 order of magnitude decrease in the transfection efficiency was observed for B-PEI/pDNA polyplexes after preincubation with 20% serum probably due to the nonspecific interaction of the cationic polyplexes with negatively charged biomacromolecules, inducing the decrease in the cellular uptake. In a sharp contrast, the polyplex micelle sytems still retained sufficient transfection efficiency toward HuH-7 cells even after preincubation with 20% serum. The almost neutral surface charge ($\zeta \sim +5$ mV in Table 1) of the Lac-PEG-PSAO-PAMA/pDNA polyplex micelles with the highly lactosylated PEG outer shell surrounding the PIC core and the PSAO inner shell may induce the micelles to tolerate serum components, allowing the cellular specific interaction through ASGP receptor-mediated endocytosis to retain efficiency even after the serum preincubation.

CONCLUSIONS

In conclusion, this study demonstrates the pH-responsive nature of novel three-layered polyplex micelles composed of a lactosylated-PEG-PSAO-PAMA triblock copolymer and pDNA, aimed at the development of a targetable and endosome-disruptive gene delivery system. The Lac-PEG-PSAO-PAMA triblock copolymer bearing a PAMA segment as the DNA-condensing polyamine and a PSAO segment as the pH-responsive polyamine was successfully synthesized. The Lac-PEG-PSAO-PAMA triblock copolymer, thus prepared, spontaneously associated with pDNA to form three-layered polyplex micelles with a PAMA/pDNA PIC core, a free PSAO inner shell, and a lactosylated PEG outer shell, as confirmed by ^{1}H NMR spectroscopy. Under physiological conditions, the Lac-PEG-PSAO-PAMA/pDNA polyplex micelles prepared at an N/P ratio above 3 were found to be able to condense pDNA (EtBr assay), thus forming polyplex micelles with a relatively small size (< 150 nm, DLS measurements), and an almost neutral surface charge ($\zeta \sim +5$ mV, zeta-potential measurements). The Lac-PEG-PSAO-PAMA/pDNA polyplex micelle formed at N/P = 3 exhibited a pH-induced size variation (pH = 7.4, 132.6 nm → pH = 4.0, 181.8 nm) corresponding to the conformational changes (globule-rod transition) in the uncomplexed PSAO chain in response to pH. The swelling of the free PSAO inner shell is likely to occur in this process while retaining the condensed PIC core composed of the PAMA segment and pDNA. The fluorescence microscopic observation revealed that the interaction of the polyplex micelle entrapping FITC-labeled pDNA with HuH-7 cells was significantly reduced in the presence of ASF compared to the condition without ASF, suggesting that ASGP receptor-mediated endocytosis would be a major route of the cellular uptake of the Lac-PEG-PSAO-PAMA/pDNA polyplex micelles. Furthermore, the Lac-PEG-PSAO-PAMA/pDNA polyplex micelles exhibited more efficient transfection ability than Lac-PEG-PSAO/pDNA and Lac-PEG-PAMA/pDNA polyplex micelles. Presumably, the Lac-PEG-PSAO-PAMA/pDNA polyplex micelles might have an endosomal escape function, and thus, hydroxychloroquine as an endosomolytic agent was not required to observe appreciable transfection. Several important factors are likely to be synergistically involved in the pronounced transfection efficiency of the Lac-PEG-PSAO-PAMA/pDNA polyplex micelles, such as minimal interaction with serum proteins, enhancement of the cellular uptake through ASGP receptor-mediated endocytosis, and effective transport to the cytoplasm from the endosomal compartment (endosomal escape). Therefore, the polyplex micelle composed of the ABC triblock copolymer, thus described here, would be a promising vector for smart gene delivery.

ACKNOWLEDGMENT

This work was supported by the Core Research for Evolutional Science and Technology (CREST) from the Japan Science and Technology Agency [JST]. We thank Professor Dr. Teiji Tsuruta for helpful comments on the preparation of the manuscript and Hiroshi Ogawa for the excellent experimental support.

Supporting Information Available: Other experimental procedures and results including synthesis of PEGs, the ^{1}H NMR spectrum of polyplex micelles at pD 4.0, and the MTT assay. This material is available free of charge via the Internet at http://pubs.acs.org.

LITERATURE CITED

(1) Yang, Y., Li, Q., Ertl, H. C., and Wilson, J. M. (1995) Cellular and humoral immune response to viral antigens create barrier to lung-directed gene therapy with recombinant adenoviruses. *J. Virol. 69*, 2004−2015.

(2) Yang, Y., Li, Q., Ertl, H. C., and Wilson, J. M. (1994) MHC class I-restricted cytotoxic T lymphocytes to viral antigens destroy hepatocytes in mice infected with E1-deleted recombinant adenoviruses. *Immunity 1*, 433−442.

(3) Gunter, K. C., Khan, A. S., and Noguchi, P. D. (1993) The safety of retroviral vectors. *Hum. Gene Ther. 4*, 643−645.

(4) Wakebayashi, D., Nishiyama, N., Itaka, K., Miyata, K., Yamasaki, Y., Harada, A., Koyama, H., Nagasaki, Y., and Kataoka, K. (2004) Polyion complex micelles of pDNA with acetal-poly(ethylene glycol)-poly(2-(dimethylamino)ethyl methacrylate) block copolymer as the gene carrier system: physicochemical properties of micelles relevant to gene transfection efficacy. *Biomacromolecules 5*, 2128−2136.

(5) Itaka, K., Yamauchi, K., Harada, A., Nakamura, K., Kawaguchi, H., and Kataoka, K. (2003) Polyion complex micelles from plasmid DNA and poly(ethylene glycol)-poly(L-lysine) block copolymer as serum-tolerable polyplex system: physicochemical properties of micelles relevant to gene transfection efficiency. *Biomaterials 24*, 4495−4506.

(6) Itaka, K., Yamauchi, K., Harada, A., Nakamura, K., Kawaguchi, H., and Kataoka, K. (2002) Evaluation by fluorescence resonance energy transfer of the stability of nonviral gene delivery vectors under physiological conditions. *Biomacromolecules 3*, 841−845.

(7) Harada-Shiba, M., Yamauchi, K., Harada, A., Takamisawa, I., Shimokado, K., and Kataoka, K. (2002) Polyion complex micelles as vectors in gene therapy-pharmacokinetics and in vivo gene transfer. *Gene Therapy 9*, 407−417.

(8) Kataoka, K., Harada, A., Wakebayashi, D., and Nagasaki, Y. (1999) Polyion complex micelles with reactive aldehyde groups on their surface from plasmid DNA and end-functionalized charged block copolymers. *Macromolecules 32*, 6892−6894.

(9) Katayose, K., and Kataoka, K. (1998) Remarkable increase in nuclease resistance of plasmid DNA through supramolecular assembly with poly(ethylene glycol)-poly(L-lysine) block copolymer. *J. Pharm. Sci. 87*, 160−163.

(10) Katayose, S., and Kataoka, K. (1997) Water-soluble polyion complex associates of DNA and poly(ethylene glycol)-poly(L-lysine) block copolymer. *Bioconjugate Chem. 8*, 702−707.

(11) Wakebayashi, D., Nishiyama, N., Yamasaki, Y., Itaka, K., Kanayama, N., Harada, A., Nagasaki, Y., and Kataoka, K. (2004) Lactose-conjugated polyion complex micelles incorporating plasmid DNA as a targetable gene vector system: their preparation and gene transfecting efficiency against cultured HepG2 cells. *J. Control. Release 95*, 653−664.

(12) van de Wetering, P., Cherng, J. Y., Talsma, H., Crommelin, D. J. A., and Hennink, W. E. (1998) 2-(Dimethylamino)ethyl methacrylate based (co)polymers as gene transfer agents. *J. Control. Release 53*, 145−153.

(13) Cherng, J. Y., Van de Wetering, P., Tslsma, H.; Crommelin, D. J. A., and Hennink, W. E. (1996) Effect of size and serum proteins on transfection efficiency of poly ((2-dimethylamino)ethyl methacrylate)-plasmid nanoparticles. *Pharm. Res. 13*, 1038−1042.

(14) Brown, M. D., Schatslein, A. G., and Uchegbu, I. F. (2001) Gene delivery with synthetic (non viral) carriers. *Int. J. Pharm. 229*, 1−21.

(15) Nishikawa, M., and Huang, L. (2001) Nonviral vectors in the new millennium: delivery barriers in gene transfer. *Hum. Gene Ther. 12*, 861−870.

(16) Lloyd, J. B. (2000) Lysosome membrane permeability: implications for drug delivery. *Adv. Drug Deliv. Rev. 41*, 189−200.

(17) Gruenberg, J. (2001) The endocytic pathway: a mosaic of domains. *Nat. Rev.: Mol. Cell. Biol. 2*, 721−730.

(18) Clague, M. J. (1998) Molecular aspects of the endocytic pathway. *Biochem. J. 336*, 271−282.

(19) Mukherjee, S., Ghosh, R. N., and Maxfield, F. R. (1997) Endocytosis. *Physiol. Rev. 77*, 759−803.

(20) Duncan, R. (1992) Drug-polymer conjugates: potential for improved chemotherapy. *Anti-Cancer Drugs 3*, 175−210.

(21) Boussif, O., Lezoualc, F., Zanta, M. A., Mergny, M. D., Scherman, D., Demeneix, B., and Behr, J. P. (1995) A versatile vector for gene

and oligonucleotide transfer into cells in culture and in vivo: polyethylenimine. *Proc. Natl. Acd. Sci. U.S.A. 92*, 7297−7301.
(22) Kabanov, A. V., Bronich, T. K., Kabanov, V. A., Yu, K., and Eisenberg, A. (1998) Soluble stoichiometric complexes from poly(*N*-ethyl-4-vinylpyridinium) cations and poly(ethylene oxide)-*block*-polymethacrylate anions. *Macromolecules 29*, 6797−6802.
(23) Fukushima, S., Miyata, K., Nishiyama, N., Kanayama, N., Yamasaki, Y., and Kataoka, K. (2005) PEGylated polyplex micelles from triblock catiomers with spatially ordered layering of condensed pDNA and buffering units for enhanced intracellular gene delivery. *J. Am. Chem. Soc. 127*, 2810−2811.
(24) Nagasaki, Y., Luo, L. B., Tsuruta, T., and Kataoka, K. (2001) Novel pH-sensitive poly(silamine) hydrogel microsphere possessing a stable skin layer. *Macromol. Rapid Commun. 22*, 1124−1127.
(25) Luo, L. B., Kato, M., Tsuruta, T., Kataoka, K., and Nagasaki, Y. (2000) Stimuli-sensitive polymer gels that stiffen upon swelling. *Macromolecules 33*, 4992−4994.
(26) Nagasaki, Y., Kazama, K., Honzawa, E., Kato, M., Kataoka, K., and Tsuruta, T. (1996) A hydrogel with rubber elasticity transition. *Macromol. Symp. 109*, 27−40.
(27) Nagasaki, Y., Kazama, K., Honzawa, E., Kato, M., Kataoka, K., and Tsuruta, T. (1995) Rubber elasticity transition of poly(silamine) induced by ionic interactions. *Macromolecules 28*, 8870−8871.
(28) Nagasaki, Y., Honzawa, E., Kato, M., and Kataoka, K. (1994) Novel stimuli-sensitive telechelic oligomers. pH and temperature sensitivities of poly(silamine) oligomers. *Macromolecules 27*, 4848−4850.
(29) Nagasaki, Y., Honzawa, E., Kato, M., Kihara, Y., and Tsuruta, T. (1992) Novel synthesis of a macromonomer having organosilyl and amino groups. *J. Macromol. Sci., Pure Appl. Chem. A29*, 457−470.
(30) van de Wetering, P., Schuurmans-Nieuwenbroek, N. M. E., Hennink, W. E., and Storm. G. (1999) Comparative transfection studies of human ovarian carcinoma cells in vitro, ex vivo and in vivo with poly(2-(dimethylamino)ethyl methacrylate)-based polyplexes. *J. Gene Med. 1*, 156−165.
(31) Cherng, J. Y., Talsma, H., Verrijik, R., Crommelin, D. J., and Hennink, W. E. (1999) The effect of formulation parameters on the size of poly-((2-dimethylamino)ethyl methacrylate)-plasmid complexes. *Eur. J. Pharm. Biopharm. 47*, 215−224.
(32) Nagasaki, Y., Sato, Y., and Kato, M. (1997) A novel synthesis of ssemitelechelic functional poly(methacrylate)s through an alcoholate-initiated polymerization. Synthesis of poly[2-(N,N-diethylaminoethyl) methacrylate] macromonomer. *Macromol. Rapid Commun. 18*, 827−835.
(33) Kitano, H., Shoda, K., and Kosaka, A. (1995) Galactose-containing amphiphiles prepared with a lipophilic radical initiator. *Bioconjugate Chem. 6*, 131−134.
(34) Hashida, M., Takemura, S., Nishikawa, M., and Takakura, Y. (1998) Targeted delivery of plasmid DNA complexed with galactosylated poly(L-lysine). *J. Controlled Release 53*, 301−310.
(35) Stockert, R. J. (1995) The asialoglycoprotein receptor: relationships between structure, function, and expression. *Physiol. Rev. 75*, 591−609.
(36) Zanta, M. A., Boussif, O., Adib, A., and Behr, J. P. (1997) In vitro gene delivery to hepatocytes with galactosylated polyethylenimine. *Bioconjugate Chem. 8*, 839−844.
(37) Plank, C., Mechter, K., Szoka, F. C., Jr., and Wagner, E. (1996) Activation of the complement system by synthetic DNA complexes: a potential barrier for intravenous gene delivery. *Hum. Gene Ther. 7*, 1437−1446.
(38) Uherek, C., Fominaya, J., and Wels, W. (1998) A modular DNA carrier protein based on the structure of diphtheria toxin mediates target cell-specific gene delivery. *J. Biol. Chem. 273*, 8835−8841.

BC050364M

Intraarticular Injection of High Molecular Weight Hyaluronan for Osteoarthritis of the Knee — Prediction of Effectiveness with Biological Markers

HARUO SUGIMOTO, HARUMOTO YAMADA, NOBUKI TERADA, ARIHIKO KANAJI, SHINICHI KATO, HIDEKI DATE, HIROFUSA ICHINOSE, and KYOSUKE MIYAZAKI

Reprinted from THE JOURNAL OF RHEUMATOLOGY

Volume 33, Number 12, December 2006

Pages 2527–2531

Intraarticular Injection of High Molecular Weight Hyaluronan for Osteoarthritis of the Knee — Prediction of Effectiveness with Biological Markers

HARUO SUGIMOTO, HARUMOTO YAMADA, NOBUKI TERADA, ARIHIKO KANAJI, SHINICHI KATO, HIDEKI DATE, HIROFUSA ICHINOSE, and KYOSUKE MIYAZAKI

ABSTRACT. ***Objective.*** The possibility of predicting the effectiveness of intraarticular injection of high molecular weight hyaluronan (HA) was investigated using biological markers.

Methods. In 32 patients with osteoarthritis (OA) of the knee, 38 knees were treated with HA injection, and the clinical symptoms were evaluated using the Japanese Orthopaedic Association (JOA) score and pain visual analog scale (VAS). The concentrations of chondroitin 6-sulfate, 4-sulfate (C6S, C4S), and aggrecan were measured in synovial fluid collected at the time of initiation of injection. The relationship between the biological markers and the improvement of clinical symptoms after injection for 1 month was investigated.

Results. C6S/C4S and concentration of aggrecan decreased after injection, although these decreases were not significant. Positive correlations were noted between the concentrations of C6S and aggrecan before HA injection and the improvement of the JOA score after injection; however, radiological OA stage had no significant relation with improvement both of the JOA score and VAS.

Conclusion. It has been reported that the concentration of aggrecan-derived fragments in synovial fluid decreases with advancement of the OA stage, reflecting decreases in the amount of residual cartilage and suppression of chondrocyte metabolism. Our findings suggested that HA injection exhibits a greater clinical effect in cases with a high intraarticular aggrecan fragment concentration, i.e., cases in which a high amount of residual cartilage and chondrocyte metabolic activity remain.The biological markers were useful in predicting the effectiveness of HA injection for OA of the knee. (J Rheumatol 2006;33:2527–31)

Key Indexing Terms:
OSTEOARTHRITIS HYALURONAN SYNOVIAL FLUID
MARKER PREDICTION INTRAARTICULAR INJECTION THERAPY

The prevalence of osteoarthritis (OA) has increased markedly with the rapid shift towards the elderly in industrially advanced countries. The major lesion of OA involves degeneration and destruction of cartilage. The early process of destruction of cartilage in OA involves degradation and conversion to lower molecular weight cartilage matrix, such as type II collagen and aggrecan, that maintains the mechanical characteristics of cartilage. Cartilage matrix is degraded and converted to low molecular components mainly by proteases produced by chondrocytes, and these destructive proteases are regulated by inflammatory cytokines and growth factors.

From the Department of Orthopaedic Surgery, Fujita Health University, Second Hospital; Department of Orthopaedic Surgery, Fujita Health University; and Seikagaku Co. Ltd., Tokyo, Japan.

Supported by Seikagaku Co. Ltd.

H. Sugimoto, MD; N. Terada, MD, Associate Professor; S. Kato, MD, Department of Orthopaedic Surgery, Fujita Health University, Second Hospital; H. Yamada, MD, Professor and Chairman; A. Kanaji, MD, Lecturer; H. Date, MD; H. Ichinose, MD, Department of Orthopaedic Surgery, Fujita Health University; K. Miyazaki, Seikagaku Co. Ltd.

Address reprint requests to Prof. H. Yamada, Department of Orthopaedic Surgery, Fujita Health University, Toyoake, Aichi, 470-1192, Japan. E-mail: hayamada@fujita-hu.ac.jp

Accepted for publication July 10, 2006.

Most therapeutic drugs for OA are symptom-modifying drugs that improve the clinical symptoms of OA, such as pain. Few candidate structure-modifying drugs have been confirmed clinically to inhibit cartilage destruction, and the effectiveness of these drugs is currently being investigated in a large-scale clinical study[1,2]. One such drug therapy for OA is intraarticular injection of high molecular weight hyaluronan (HA). HA is a long linear-chain glycosaminoglycan consisting of a repetitive disaccharide unit structure that is the main component of synovial fluid. HA is important in maintaining the viscoelasticity of articular cartilage, and contributes to the maintenance of low friction, which is an important articular function, through synergistic action with cartilage. HA in synovial fluid is produced by synovial cells, and has a molecular weight of about $4–5 \times 10^6$ Da in normal subjects. In arthropathy, such as rheumatoid arthritis and OA, both the molecular weight and concentration of HA are decreased[3]. Such decreases in the molecular weight and concentration of HA impair lubrication between cartilage, decrease impact-absorbing ability, and cause further degeneration of the cartilage. HA receptors, including lymphocyte homing receptors, CD44, are present on the chondrocyte surface. In addition to the hydrody-

namic action described above, HA alters chondrocyte metabolism through receptors, and acts to protect cartilage tissue[4]. HA has been reported to exhibit cartilage-protective effects, including stimulation of chondrocyte proliferation, production of cartilage matrix, inhibition of the production of protease[5], stimulation of the production of a protease inhibitor[6], movement of newly synthesized aggrecan around chondrocyte[7], and inhibition of chondrocyte apoptosis *in vitro* [8].

HA injection improves the clinical symptoms of OA, mainly pain, in about 70% of OA cases, but nonresponders to this therapy do exist. Joint puncture is an invasive procedure that is performed with HA injection. As such, this procedure has a risk of complications, including infection. Prediction of the clinical effectiveness of this therapy enables us to perform efficient medical care.

Measurement of biological markers that are derived from components of joints, such as cartilage, synovial membrane, and bone, in synovial fluid, blood, and urine, has allowed investigation of the pathology of arthropathy[9]. Typical biological markers that reflect cartilage turnover are fragments derived from type II collagen, aggrecan, and other minor proteins that are present in cartilage. Aggrecan-derived markers are core proteins, fragments of aggrecan, glycosaminoglycans (GAG) composing aggrecan, chondroitin 6-sulfate and 4-sulfate (C6S and C4S), and keratan sulfate (KS)[10-12]. Unlike radiograph and magnetic resonance imaging, these biological markers reflect real-time metabolism of joint components, such as cartilage and synovial membrane. Our objective was to investigate the possibility of predicting the effectiveness of HA injection from biological markers in synovial fluid collected at the initiation of intraarticular injection of HA.

MATERIALS AND METHODS

Patients. The subjects were 32 outpatients with OA of the knee (38 joints) at our orthopedic outpatient clinic who had apparent pain on movement and hydrarthrosis, and were indicated for HA injection. No concomitant steroid or nonsteroidal antiinflammatory drugs (NSAID) were administered. Patients treated with HA preparations within the past 3 months and patients with suspected rheumatoid arthritis, trauma, and suppurative arthritis were excluded. The patients' characteristics are shown in Table 1.

Intraarticular injection and collection of synovial fluid. An injection containing 25 mg of HA (molecular weight of about 900,000 Da) in 2.5 ml (superpurified hyaluronate, Seikagaku Co. Ltd., Tokyo, Japan) was injected into the knee joint once a week for one month. Synovial fluid was collected at the initiation of the first injection, and centrifuged at 3000 rpm for 15 minutes at room temperature. The supernatant was collected and immediately stored at –85°C.

Evaluation by radiography. Plain radiograms of the knee (frontal and lateral views and frontal view with weight-bearing) were acquired before the initiation of injection, and the OA stage was determined based on the Koshino classification scale[13] (grade 0: normal, grade 1: osteosclerosis or osteophyte formation, grade 2: narrowing of the joint space to 3 mm or less, grade 3: disappearance of the joint space, grade 4: 5 mm or less bone defect of the weight-bearing surface, grade 5: 5 mm or more bone defect of the weight-bearing surface; Table 1).

Evaluation of clinical symptoms. Clinical evaluation of OA was performed, based on the criteria for judgment of therapeutic results of knee OA established by the Japanese Orthopaedic Association (JOA score)[14]. In this score, pain on walking, pain on ascending and descending the stairs, range of motion, and joint swelling were rated with maximum scores of 30, 25, 35, and 10, respectively. The subjective and objective symptoms were evaluated based on the JOA scores before the initiation of intraarticular injection and at 1 month after injection. Pain was evaluated using the 100 mm visual analog scale (VAS).

Table 1. Patients' characteristics. Stage of knee deformity was assessed by the radiological findings according to the Koshino criteria[13].

	n
Sex	
Male	4
Female	34
Age, yrs	
> 60	4
60–70	5
70–80	10
< 80	19
Radiological stage	(mean = 73.4 ± 8.2)
I	11
II	5
III	13
IV	5
V	4

Measurement of biological markers. C6S and C4S in synovial fluid were measured by high performance liquid chromatography according to the method reported by Shinmei, *et al*[11]. Glycosaminoglycans in synovial fluid were degraded to disaccharides by treatment with chondroitinase ABC and chondroitinase AC-II, and applied to a column packed with propylamine-bound silica gel (YMC gel PA-120; YMC, Kyoto, Japan) for quantification. The aggrecan level was measured using a sandwich ELISA measurement kit (Biosource Co.) This measurement kit uses an anti-KS monoclonal antibody for capturing and a labeled anti-G1-domain monoclonal antibody as a detector, and selectively measures aggrecan molecules with HA-binding ability and a KS side chain[15].

Statistical analysis. The results of measurement of the biological markers were presented as the means ± standard deviation. For analysis of the significance of between-group differences, paired t test or Wilcoxon signed-rank test was used. For analysis of correlation, Spearman's correlation coefficient by rank was used (StatView 5.0, Abacus Concepts Inc., Berkeley, CA, USA).

RESULTS

Time-course of changes in biological markers after injection. The C6S and C4S concentrations in synovial fluid showed no significant change after injection for 1 month. C6S/C4S and aggrecan concentration decreased over time, but the decrease was not significant (Figure 1).

Relationship between biological markers before injection and improvement of clinical symptoms. The relationships between the concentrations of the biological markers before HA injection and improvement of the JOA score and VAS one month after initiation of injection were investigated by regression analysis.

A significant positive correlation was observed between the C6S concentration before injection and improvement of the JOA score after one month ($r = 0.322$, $p = 0.0383$; Figure 2). No significant correlation was apparent between the C4S

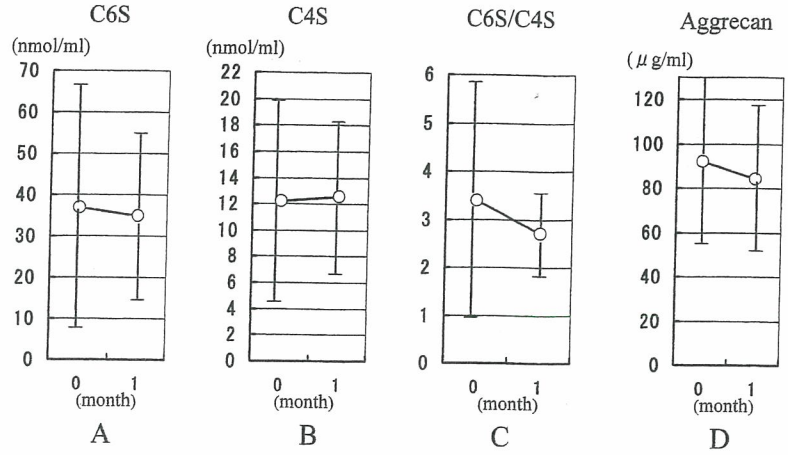

Figure 1. Time-course of changes in biological markers. HA with MW 800,000 Da was injected into the knee joint once a week for one month. C6S and C4S in synovial fluid were measured by HPLC. The aggrecan level in synovial fluid was measured using a sandwich ELISA measurement kit. Data were shown as mean ± SD. A: C6S. B: C4S. C: C6S/C4S. D: Aggrecan.

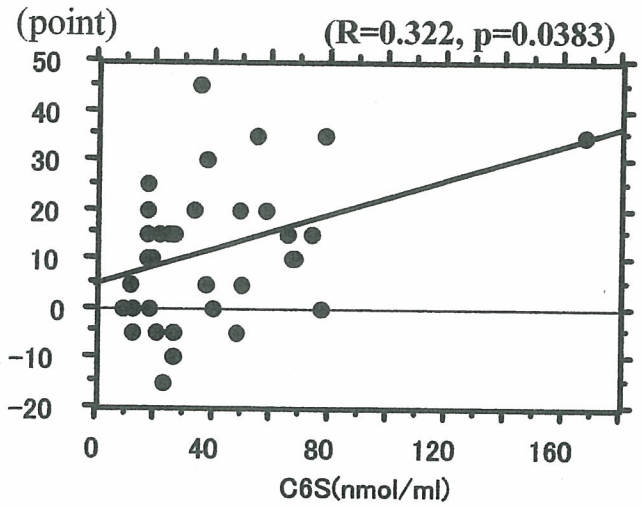

Figure 2. Relationship between C6S concentration before injection and improvement of JOA score. The relationships between C6S concentration before HA injection and improvement of the JOA score one month after initiation of injection were investigated by regression analysis.

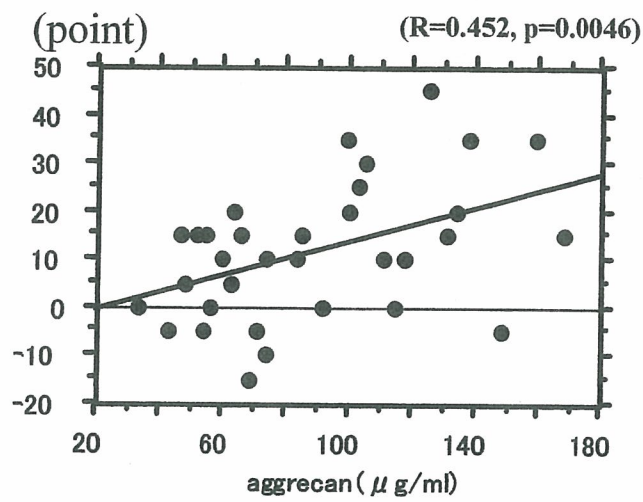

Figure 3. Relationship between aggrecan concentration before injection and improvement of JOA score. The relationships between aggrecan concentration before HA injection and improvement of the JOA score one month after initiation of injection were investigated by regression analysis.

concentration or C6S/C4S before injection and the improvement of the JOA score (data not shown). A significant correlation was observed between the aggrecan concentration before injection and improvement of the JOA score after 1 month ($r = 0.452$, $p = 0.0046$; Figure 3). In contrast, no significant correlation was apparent between the biological marker concentrations before injection and improvement of VAS (data not shown). Relationship between level of biological marker and improvement of each item of JOA score was analyzed. Significant correlation was observed between C6S concentration before injection and improvement of pain on waking ($r = 0.465$, $p = 0.0221$), and range of motion ($r = 0.433$, $p = 0.0282$) after one month. Aggrecan concentration correlated significantly with improvement of pain on walking ($r = 0.451$, $p = 0.0268$), and pain on ascending and descending the stairs ($r = 0.577$, $p = 0.0025$) after one month. OA stage determined by radiographic findings had no significant relation with improvement of both the JOA score and VAS (Figure 4).

DISCUSSION

In OA, viscoelastic substances in synovial fluid, mainly HA, become deteriorated. Intraarticular injection of HA has been initiated based on the concept of viscosupplementation: supplementation of deteriorated HA with a novel viscoelastic substance that exhibits a hydrodynamic function[16]. HA has

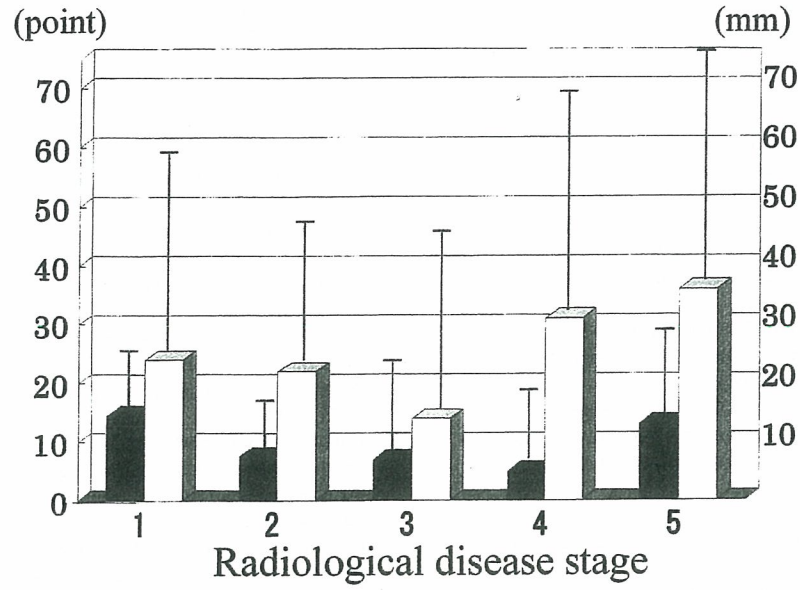

Figure 4. Radiological disease stage and improvement of JOA score and VAS. OA disease stage determined by radiographic findings had no significant relation with improvement both of the JOA score and VAS. Data were shown as mean ± SD. Black bar: JOA score (points). White bar: VAS (mm).

been considered as a symptom-modifying drug that primarily improves the pain of OA[17]. HA injection apparently improved the clinical symptoms of OA, including pain, in this study.

Cartilage markers are divided into markers of synthesis and catabolism. Typical markers of catabolism reflecting the destruction of cartilage include aggrecan molecules released from aggrecan, side chain KS, and CS. There are 2 types of CS: C6S, which is abundant in healthy cartilage, and C4S, which is abundant in degenerated cartilage as with OA[18]. Changes in joint markers during the course of treatment of OA can help in determining the effectiveness of treatment. Yamada, *et al* measured various joint markers in synovial fluid before and after HA injection into the joint in patients with knee OA, and found that the PIICP concentration increased significantly after HA injection[19]. Since PIICP is a marker of the synthesis of type II collagen[20,21], this finding suggested that HA injection promoted matrix synthesis by chondrocytes. In studies reported by Namiki, *et al*, and Uesaka, *et al*[22,23], C6S and C4S levels decreased after HA injection. In our study, aggrecan level was decreased after injection of HA for one month, but this decrease was not significant. Thus, our study did not demonstrate inhibition of the degradation of cartilage aggrecan by HA injection in OA.

There has been no report of prediction of the efficacy of intraarticular injection of HA for OA based upon biological markers. We observed a significant positive correlation between the C6S concentration before injection and improvement of the JOA score after one month of injection. Furthermore, a stronger positive correlation, compared with that of C6S, was noted between the aggrecan concentration before injection and the JOA score after one month of injection. However, radiological OA stage had no significant relation with improvement both of the JOA score and VAS. These findings suggest that improvement of the clinical symptoms after initiation of HA injection can be predicted by measurement of the fragments derived from aggrecan. Yamada, *et al* reported that the concentration of aggrecan fragments in synovial fluid decreased with the progression of OA, as a result of decreases in the amount of residual cartilage and suppression of chondrocyte metabolism with the advancement of OA[24-26]. In consideration of these observations, our findings indicate that HA injection is effective for cases with a high intraarticular level of aggrecan fragments. This reflects an early stage of OA in keeping with residual cartilage and chondrocyte metabolic activity.

REFERENCES

1. Reginster JY, Deroisy R, Rovati LC, et al. Long-term effects of glucosamine sulphate on osteoarthritis progression: a randomized, placebo-controlled clinical trial. Lancet 2001;357:251-6.
2. Richy F, Bruyere O, Ethgen O, Cucherat M, Henrotin Y, Reginster JY. Structural and symptomatic efficacy of glucosamine and chondroitin in knee osteoarthritis: a comprehensive meta-analysis. Arch Intern Med 2003;163:1514-22.
3. Dahl LB, Dahl IMS, Engstrom LA. Concentration and molecular weight of sodium hyaluronate in synovial fluid from patients with rheumatoid arthritis and other arthropathies. Ann Rheum Dis 1985;44:817-22.
4. Lisignoli G, Grassi F, Zini N, et al. Anti-Fas-induced apoptosis in chondrocytes reduced by hyaluronan: evidence for CD44 and CD54 (intercellular adhesion molecule 1) involvement. Arthritis Rheum 2001;44:1800-7.
5. Kikuchi T, Shinmei M. Effects of hyaluronan on proteoglycan metabolism of rabbit articular chondrocytes in cultures. Jpn J Rheumatol 1994;5:207-15.

6. Yasui T, Akatsuka M, Tobetto K, et al. Effects of hyaluronan on the production of stromelysin and tissue inhibitor of metalloproteinase-1 (TIMP-1) in bovine articular chondrocytes. Biomed Res 1992;13:343-8.
7. Kikuchi T, Yamada H, Fujikawa K. Effects of high molecular weight hyaluronan on the distribution and movement of proteoglycan around chondrocytes cultured in alginate beads. Osteoarthritis Cartilage 2001;9:351-6.
8. Takahashi K, Hashimoto S, Kubo T, Hirasawa Y, Lotz M, Amiel D. Effect of hyaluronan on chondrocyte apoptosis and nitric oxide production in experimentally induced osteoarthritis. J Rheumatol 2000;27:1713-21.
9. Garnero P, Rousseau JC, Delmas PD. Molecular basis and clinical use of biochemical markers on bone, cartilage, and synovium in joint diseases. Arthritis Rheum 2000;43:953-68.
10. Campion GV, McCrae F, Schnitzer TJ, Lenz ME, Dieppe PA, Thonar EJ-MA. Levels of keratan sulfate in the serum and synovial fluid of patients with osteoarthritis of the knee. Arthritis Rheum 1991;34:1254-9.
11. Shinmei M, Miyauchi S, Machida A, Miyazaki K. Quantitation of chondroitin 4-sulfate and chondroitin 6-sulfate in pathologic joint fluid. Arthritis Rheum 1992;35:1304-8.
12. Lohmander LS, Hoerrner LA, Lark MW. Metalloproteinases, tissue inhibitor, and proteoglycan fragments in knee synovial fluid in human osteoarthritis. Arthritis Rheum 1993;36:181-9.
13. Koshino T. Etiology, classifications and clinical findings of osteoarthritis of the knee [Japanese]. Ryumachi 1985;25:191-203.
14. The Japanese Orthopaedic Association Japanese Knee Society. Assessment criteria for knee diseases and treatments. Tokyo: Kanehara, 1994.
15. Guerne PA, Desgeorges A, Jaspar JM, et al. Effects of IL-6 and its soluble receptor on proteoglycan synthesis and NO release by human articular chondrocytes: comparison with IL-1. Modulation by dexamethasone. Matrix Biology 1999;18:253-60.
16. Peyron JG, Balazs LA. Preliminary clinical assessment of Na-hyaluronate injection into human arthritic joints. Pathol Biol 1974;22:731-6.
17. Altman RD. Intra-articular sodium hyaluronate in osteoarthritis of the knee. Semin Arthritis Rheum 2000;30:11-8.
18. Mankin HJ, Lippello L. The glycosaminoglycans of normal and arthritic cartilage. J Clin Invest 1971;50:1712-9.
19. Yamada H, Yoshihara Y, Kobayashi T, et al. Intra-articular injection therapy with high-molecular weight hyaluronan for osteoarthritis of the knee joint—Effects on joint fluid markers. Orthopaedics International Edition 1997;5:117-21.
20. Shinmei M, Ito K, Matsuyama S, Yoshihara Y, Matsuzawa K. Joint fluid carboxy-terminal type II procollagen peptide as a marker of cartilage collagen biosynthesis. Osteoarthritis Cartilage 1993;1:121-8.
21. Sugiyama S, Itokazu M, Suzuki Y, Shimizu K. Procollagen II C propeptide level in the synovial fluid as a predictor of radiographic progression in early knee osteoarthritis. Ann Rheum Dis 2003;62:27-32.
22. Namiki O, Kuriyama S, Maeda H, Sakamoto A. Biochemical analysis of synovial fluid and their alteration in intra-articular injection therapy of sodium hyaluronate in osteoarthritis. Joint Surgery 1994; 21:131-7.
23. Uesaka S, Takeuchi T, Ide K, Yoshihara K, Nakayama Y, Shirai Y. Intra-articular injection therapy with sodium hyaluronate for osteoarthritis of the knee—Correlation between radiographic prognosis of osteoarthritis, joint markers and clinical evaluations. Joint Surgery 1999;26:106-12.
24. Yamada H, Miyauchi S, Hotta H, et al. Levels of chondroitin sulfate isomers in the synovial fluids from patients with hip osteoarthritis. J Orthop Science 1999;4:250-4.
25. Yamada H, Miyauchi S, Morita M, et al. Content and sulfation pattern of keratan sulfate in hip osteoarthritis using high performance liquid chromatography. J Rheumatol 2000;27:1721-4.
26. Kato S, Yamada H, Terada N, et al. Joint biomarkers in idiopathic femoral head osteonecrosis: comparison with hip osteoarthritis. J Rheumatol 2005;32:1518-23.

J|A|C|S
COMMUNICATIONS

Published on Web 04/12/2006

Semipermeable Polymer Vesicle (PICsome) Self-Assembled in Aqueous Medium from a Pair of Oppositely Charged Block Copolymers: Physiologically Stable Micro-/Nanocontainers of Water-Soluble Macromolecules

Aya Koide,[†] Akihiro Kishimura,[†,‡,§] Kensuke Osada,[†,§] Woo-Dong Jang,[†,‡,||] Yuichi Yamasaki,[†,‡,§] and Kazunori Kataoka*[,†,‡,§]

Department of Materials Engineering, Graduate School of Engineering, and Center for NanoBio Integration, The University of Tokyo, 7-3-1 Hongo, Bunkyo-ku, Tokyo 113-8656 Japan, and CREST, Japan Science and Technology Agency, Japan

Received November 24, 2005; E-mail: kataoka@bmw.t.u-tokyo.ac.jp

Polymer vesicles enclosing a volume with a molecularly thin membrane, known as "polymersomes", have recently been attracting progressive attention from both fundamental and applied standpoints as carriers or containers for various functionality compounds.[1,2] Particularly, in an aqueous entity, amphiphilic block copolymers have been used for the preparation of polymersomes,[1−3] revealing unique characteristics such as high structural stability compared to conventional liposomes made from low molecular amphiphiles.[1] Very recently, stable encapsulation of biologically relevant substances, including drugs and enzymes, into the polymersomes has been directed to applications as delivery and bioreactor systems.[2] Nevertheless, the hydrophobic nature of the membrane in such amphiphilic polymersomes prevents the penetration of hydrophilic solutes, limiting their functionality as semipermeable container systems. Furthermore, the harsh preparation conditions, including the use of organic solvents, may hamper the encapsulation of fragile compounds such as proteins. Herein, we report for the first time the preparation of stable polymersomes with a semipermeable membrane through a simple mixing of a pair of oppositely charged block copolymers in an aqueous medium. The polymersome formed in this way is a new entity of polymer vesicles with a polyion complex (PIC) membrane and thus may be given a new terminology as a "PICsome".

A PICsome as a hollow sphere needs the formation of a stable layer of PIC lamellae as the partition membrane. In this regard, oppositely charged segments of the block copolymer pair are preferred to have a matched chain length, compensating for the counter charge in a stoichiometric manner and minimizing the phase mixing of the PIC middle layer with the outer and inner shell layers of the hydrophilic segment, in this case, poly(ethylene glycol) (PEG). Here, to satisfy this condition of matched chain length, both anionic and cationic block copolymers were prepared from the same platform polymer, PEG-poly(β-benzyl-L-aspartate) (PEG-PBLA), to have identical molecular weight and composition (Scheme 1). Two types of PEG-PBLA with a different PBLA composition (degree of polymerization (DP) of PBLA; 17 and 100) were prepared by the ring opening polymerization of β-benzyl-L-aspartate *N*-carboxyanhydride initiated from the ω-primary amino group of $CH_3O-PEG-NH_2$ (M_n = 2000, M_w/M_n = 1.05).[4] The anionic component of the PICsome, PEG-poly(α,β-aspartic acid) (PEG-P(Asp)$_{17}$ and PEG-P(Asp)$_{100}$), was obtained from PEG-PBLA by alkali hydrolysis as reported previously.[5] Alternatively, the cationic

Scheme 1. Synthesis of a Pair of Oppositely Charged Block Copolymers

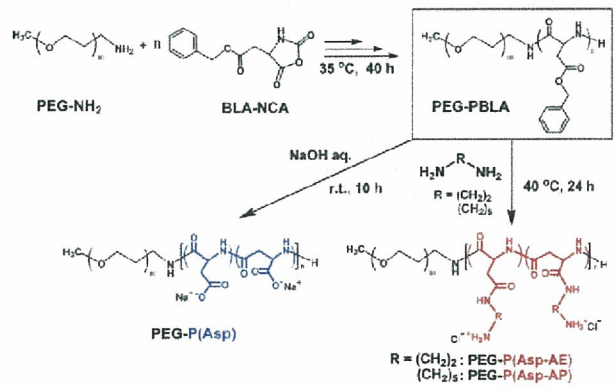

component was prepared from PEG-PBLA by aminolysis of flanking benzyl ester groups with an excess amount of diamine. A notable property of PBLA is that the benzyl ester groups can easily undergo quantitative aminolysis reactions with various diamines at ambient temperature via the formation of a succinimidyl ring structure as an intermediate, allowing the preparation of cationic poly(aspartamide)s with different amine functionalities. Indeed, quantitative aminolysis was confirmed from ^{1}H NMR spectra.[4] Two types of diamines with a different number of methylene units, 1,2-diaminoethane and 1,5-diaminopentane, were used in the aminolysis to obtain PEG-poly([2-aminoethyl]-α,β-aspartamide) (PEG-P(Asp-AE)$_{17}$ and PEG-P(Asp-AE)$_{100}$) and PEG-poly([5-aminopentyl]-α,β-aspartamide) (PEG-P(Asp-AP)$_{17}$ and PEG-P(Asp-AP)$_{100}$), respectively, to explore the effect of the alkyl-spacer length on the self-assembly behavior.

The anionic and cationic block copolymers were separately dissolved in 10 mM Tris-HCl buffer (pH 7.4) with a physiological salt concentration of 150 mM NaCl. Both solutions were then mixed in an equal ratio of $-COO-$ and $-NH_3^+$ units to form PIC and subsequently subjected to sonication.[4] Flow particle image analysis[4] and dark-field microscopic (DFM) observation suggested the formation of spherical particles with the diameter up to 10 μm in the PEG-P(Asp)$_{100}$/PEG-P(Asp-AP)$_{100}$ system (Figure 1), which is obviously with a larger size range than that of the well-documented PIC micelles with a core−shell architecture.[6] The DFM image was more fascinating, showing characteristic ringlike scatterings (Figure 1), suggesting the hollow structure of the particles. Note that the scattering light intensity in DFM correlates with the density of the objects, giving a ringlike image for hollow particles with a large density difference between the inner and peripheral regions.[7] The

[†] Department of Materials Engineering, Graduate School of Engineering, The University of Tokyo.
[‡] CREST, Japan Science and Technology Agency.
[§] Center for NanoBio Integration, The University of Tokyo.
[||] Present address: Department of Chemistry, Yonsei University, Korea.

10.1021/ja057993r CCC: $33.50

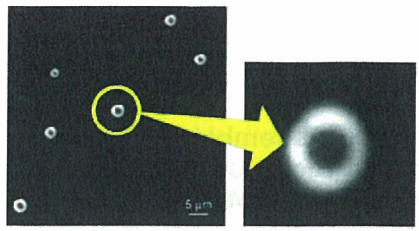

Figure 1. Dark-field microscopic images of PICsomes prepared from a PEG-P(Asp)$_{100}$/PEG-P(Asp-AP)$_{100}$ system.

balance of the segment length in the block copolymer is expected to play a substantial role in the self-assembly process. Indeed, the combination of the block copolymers with a shorter charged segment, PEG-P(Asp)$_{17}$/PEG-P(Asp-AP)$_{17}$ system, gave a DFM image with only few ring-scattering objects dispersed in the major part of the small dot scatterings presumably from micelles. Block copolymers with shorter charged segments compared to the PEG segment adopt a cone-shaped conformation preferring the micelle architecture.[6] The molecular shape gradually changes from cone to rod with the increased length of the charged segments relative to the PEG segments, and eventually, the assembly should adopt the vesicular structure with a smaller curvature than the spherical micelle.[8] The observations here are consistent with this general rule of vesicular formation through molecular assembly. Another factor influencing the vesicular formation seems to be the alkyl-spacer length of the cationic side chain of the poly(aspartamide) segment, which may be related to the flexibility of the ion pair formed in the PIC structure. A decrease in the alkyl-spacer length from pentyl to ethyl in the side chain of the cationic poly(aspartamide) segment, viz. the PEG-P(Asp)$_{100}$/PEG-P(Asp-AE)$_{100}$ system, resulted in a significant decrease in the size (<1 μm) of the ring scatterings observed in DFM. It is likely that the length of the alkyl spacer may be a critical factor in determining the stable PICsome size, yet a further detailed study should be needed to confirm this assumption.

The hollow structure of the large PIC assembly from PEG-P(Asp)$_{100}$/PEG-P(Asp-AP)$_{100}$ system as "PICsome" was further directly evidenced from the encapsulation of the water-soluble macromolecule labeled with fluorescein isothiocyanate, FITC-dextran (FITC-Dex, M_n = 40 000), into the PICsome. Cross-sectional observation by the confocal laser scanning microscope (CLSM) clearly confirmed the successful inclusion of FITC-Dex into the PICsome by a simple mixing of PEG-P(Asp-AP)$_{100}$ (1 mg/mL) with PEG-P(Asp)$_{100}$ (1 mg/mL) containing FITC-Dex (1 mg/mL) (Figure 2).[4] The PICsome with encapsulating FITC-Dex was appreciably stable in physiological buffer as observed by CLSM even after 3 months standing at ambient temperature.

The semipermeability of the PICsome membrane was then investigated using fluorescent molecules with different molecular weights. The fluorescence collected through the objective lens was resolved by the diffraction grating and monitored by a 32-channel arrayed detector. Upon addition of dextran labeled with tetramethylrhodamine isothiocyanate (TRITC-Dex, M_n = 70 000) to the solution of PICsome with encapsulated FITC-Dex, a green fluorescence of FITC inside the PICsome was clearly observed, sharply discriminated from the red fluorescence of TRITC-Dex in the outer medium, in the merged image of CLSM taken at the excitation wavelength for FITC and TRITC (488 and 543 nm) (Figure 2a). On the other hand, upon addition of free TRITC (MW = 443.5) to the solution of the FITC-Dex encapsulating PICsome, a yellow color was observed inside the PICsome (Figure 2b).[4] An emission spectrum of the region of interest (ROI) in Figure 2b shows the

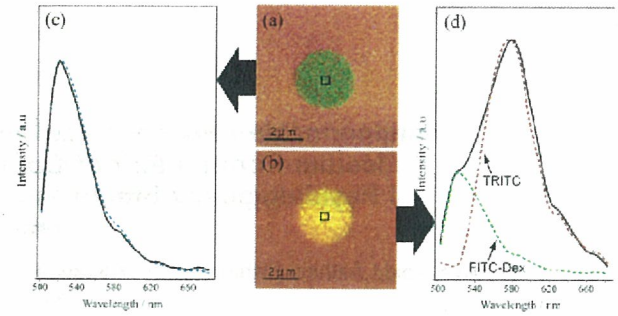

Figure 2. CLSM images and emission spectra of PICsome encapsulating FITC-Dex. Images after the addition of (a) TRITC-Dex or (b) TRITC. (c) Spectra of the ROI in (a) after (solid line) and before (blue dotted line) the addition of TRITC-Dex. (d) A spectrum of the ROI in (b) (solid line) with reference spectra of FITC-Dex (green dotted line) and TRITC (red dotted line).

intense fluorescence with the maximum at 580 nm and the shoulder at 520 nm (Figure 2d). The profile was reasonably fitted with both references of FITC-Dex and TRITC, indicating the penetration of TRITC into the PICsome interior. In contrast, the spectrum of the ROI in Figure 2a corresponds to the spectrum of FITC-Dex before the addition of TRITC-Dex (Figure 2c), indicating the segregation of TRITC-Dex from the PICsome interior. These results visually demonstrated the semipermeable character of the PIC membrane. Notably, the PICsome was able to retain its vesicular structure in the presence of a colloidal osmotic pressure of approximately 10 μOsm from the encapsulated FITC-Dex and was stable even in the medium containing 10% fetal bovine serum at 37 °C,[4] being feasible for biomedical applications.

In summary, a novel entity of a polymer vesicle, a PICsome, was prepared here by a simple mixing of a pair of oppositely charged block copolymers composed of biocompatible PEG and poly(amino acid)s in an aqueous medium. The PICsome is stable in proteinous medium and has a partition membrane with a unique three-layered structure. These biocompatible composition and biologically relevant characteristics of the PICsomes may open their future utility in biomedical fields such as carriers of therapeutic compounds and compartments for diagnostic enzymes.

Acknowledgment. We thank Prof. K. Akiyoshi and Dr. S. M. Nomura (Tokyo Medical and Dental University) for valuable suggestions for DFM observation and Mr. F. Ishidate (Carl Zeiss Co., Ltd.) for emission spectrum measurements.

Supporting Information Available: Syntheses, characterizations, and preparations of PICsomes. This material is available free of charge via the Internet at http://pubs.acs.org.

References

(1) (a) Discher, D. E.; Eisenberg, A. *Science* **2002**, *297*, 967−973. (b) Geng, Y.; Ahmed, F.; Bhasin, N.; Discher, D. E. *J. Phys. Chem. B* **2005**, *109*, 3772−3779. (c) Antonietti, M.; Förster, S. *Adv. Mater.* **2003**, *15*, 1323−1333.
(2) Brož, P.; Benito, S. M.; Saw, C.-L.; Burger, P.; Heider, H.; Pfisterer, M.; Marsch, S.; Meier, W.; Hunziker, P. *J. Control. Release* **2005**, *102*, 475−488. (b) Ranquin, A.; Versées, W.; Meier, W.; Steyaert, J.; Van Gelder, P. *Nano Lett.* **2005**, *5*, 2220−2224.
(3) (a) Bellomo, E. G.; Wyrsta, M. D.; Pakstis, L.; Pochan, D. J.; Deming, T. J. *Nat. Mater.* **2004**, *3*, 244−248. (b) Rodoríguez-Hernández, J.; Lecommandoux, S. *J. Am. Chem. Soc.* **2005**, *127*, 2026−2027.
(4) See Supporting Information.
(5) Yokoyama, M.; Inoue, S.; Kataoka, K.; Yui N.; Okano, T.; Sakurai, Y. *Makromol. Chem.* **1989**, *190*, 2041−2054.
(6) (a) Harada, A.; Kataoka, K. *Macromolecules* **1995**, *28*, 5294−5299. (b) Harada, A.; Kataoka, K. *Science* **1999**, *283*, 65−67. (c) Kataoka, K.; Harada, A.; Nagasaki, Y. *Adv. Drug Delivery Rev.* **2001**, *47*, 113−131.
(7) Hotani, H. *J. Mol. Biol.* **1984**, *178*, 113−120.
(8) Zhang, L.; Eisenberg, A. *J. Am. Chem. Soc.* **1996**, *118*, 3168−3181.

JA057993R

Available online at www.sciencedirect.com
SCIENCE DIRECT
Journal of Controlled Release 113 (2006) 73–79
journal of controlled release
www.elsevier.com/locate/jconrel

Polyion complex micelles for photodynamic therapy: Incorporation of dendritic photosensitizer excitable at long wavelength relevant to improved tissue-penetrating property

Woo-Dong Jang [a,d,1], Yoshinori Nakagishi [c], Nobuhiro Nishiyama [b], Satoko Kawauchi [c], Yuji Morimoto [c], Makoto Kikuchi [c], Kazunori Kataoka [a,b,d,e,*]

[a] *Department of Materials Engineering, Graduate School of Engineering, The University of Tokyo, 7-3-1 Hongo, Bunkyo-ku, Tokyo 113-8656, Japan*
[b] *Center for Disease Biology and Integrative Medicine, The University of Tokyo, 7-3-1 Hongo, Bunkyo-ku, Tokyo, 113-8656, Japan*
[c] *Department of Medical Engineering, National Defense Medical College, 3-2 Namiki, Tokorozawa, Saitama, 359-8513, Japan*
[d] *Core Research for Evolutional Science and Technology (CREST), Japan Science and Technology Agency (JST), Japan*
[e] *Center for NanoBio Integration, The University of Tokyo, 7-3-1 Hongo, Bunkyo-ku, Tokyo, 113-8656, Japan*

Received 29 October 2005; accepted 10 March 2006
Available online 15 May 2006

Abstract

A polymeric micelle (DPcZn/m) system, which is formed via an electrostatic interaction of anionic dendrimer phthalocyanine (DPcZn) and poly(ethylene glycol)-poly(L-lysine) block copolymers (PEG-*b*-PLL), was prepared for use as an effective photosensitizer for photodynamic therapy. DPcZn/m exhibited strong Q band absorption around 650 nm, a useful wavelength for high tissue penetration. Dynamic light scattering studies indicated that the DPcZn/m system has a relevant size of 50 nm for intravenous administration. Under light irradiation, either DPcZn or DPcZn/m exhibited efficient consumption of dissolved oxygen in a medium to generate reactive oxygen species and an irradiation-time-dependent increase in photocytotoxicity. The photodynamic efficacy of the DPcZn was drastically improved by the incorporation into the polymeric micelles, typically exhibiting more than two orders of magnitude higher photocytotoxicity compared with the free DPcZn at 60-min photoirradiation.

Keywords: Dendrimer; Photosensitizer; Phthalocyanine; Polymeric micelle; Photodynamic therapy

1. Introduction

Photodynamic therapy is based on the accumulation of a photosensitizer in malignant tissue after its administration usually through intravenous route [1–5]. Subsequent illumination with laser light of an appropriate wavelength generates reactive oxygen species (ROS) which results in tissue destruction. For an effective photodynamic effect, several ideal properties of photosensitizers should be needed. From the chemical point of view, the materials should be pure and have a high quantum yield of singlet oxygen generation. From the biological point of view, it should have no dark toxicity and have high solubility in an aqueous medium for the easy administration. High tumor localization and long wavelength absorption are also very important for effective medical treatment.

In this context, we have recently reported ionic dendrimer porphyrin as an efficient photosensitizer for photodynamic therapy [6–9]. To obtain high quantum yields and effective energy absorption, photosensitizers must generally have large π-conjugation domains. Therefore, most of photosensitizers easily form aggregates, which provide a self-quenching effect of the excited state in aqueous medium due to their π–π interaction and hydrophobic characteristics [10,11]. To overcome these problems, the structure of ionic dendrimer porphyrin is promising, because the substitution of large dendritic wedges

* Corresponding author. Department of Materials Engineering, Graduate School of Engineering, The University of Tokyo, 7-3-1 Hongo, Bunkyo-ku, Tokyo 113-8656, Japan. Tel.: +81 3 5841 7138; fax: +81 3 5841 7139.
E-mail address: kataoka@bmw.t.u-tokyo.ac.jp (K. Kataoka).
[1] Current address: Department of Chemistry, Collage of Science, Yonsei University, 134 Sinchondong, Seodaemun-gu, Seoul 120-749, Korea.

0168-3659/$ - see front matter © 2006 Elsevier B.V. All rights reserved.
doi:10.1016/j.jconrel.2006.03.009

sufficiently prevents the formation of aggregates and provides high solubility in the aqueous medium. Furthermore, a charged ion surface can form polyion complex micelles by means of electrostatic interaction with an oppositely charged block copolymer. These types of polyion complex micelles [12] with a PEG shell were demonstrated to accumulate effectively and specifically in solid tumor tissue due to the hyperpermeability of tumor capillaries. However, the dendrimer porphyrin has a relatively short wavelength absorption, where the absorption maximum is 430 nm, which is a limitation to improvement for practical PDT application. In relation to this fact, several phthalocyanine molecules, including the one with a dendritic architecture, are of interest as a potential photosensitizer with appropriate wavelength absorption for practical PDT application [13–16]. Herein, we report the first example of dendritic phthalocyanine-incorporated polyion complex micelle formation and demonstrate an order-of-magnitude enhancement in photodynamic efficacy of the phthalocyanine dendrimer through the micelle encapsulation at an excitation wavelength with clinical relevance (~600 nm).

2. Materials and methods

2.1. Materials

N^{ε}-Z-L-lysine and bis(trichloromethyl) carbonate (triphosgene), for the synthesis of polyethylene glycol-block-poly-L-lysine (PEG-*b*-PLL), were purchased from Tokyo Kasei Co., Ltd. α-Methoxy-ω-amino-poly(ethylene glycol) (MeO-PEG-NH_2, Mw = 12 kg/mol) was a kind gift from Nippon Oil and Fats Co., Ltd. Chemicals for dendrimer synthesis were purchased from Tokyo Kasei Co., Ltd. or Aldrich Chemical Co., Ltd. Tetrahydrofuran and hexane, used as a solvent for the synthetic reactions, were distilled from sodium benzophenone ketyl under Ar just before use. *n*-Pentanol and 1,8-diazabicyclo-(5,4,0)-undec-7-ene (DBU) for phthalocyanine dendrimer synthesis, were used as received without further purification.

2.2. Synthesis of block copolymer

MeO-PEG-NH_2 was precipitated in diethylether from chloroform, dried under reduced pressure and subsequently freeze-dried from benzene prior to use in the block copolymer synthesis. PEG-*b*-PLL was synthesized by a previously reported procedure [17]. Briefly, the *N*-carboxy anhydride of N^{ε}-Z-L-lysine was polymerized by initiation with CH_3O-PEG-NH_2 (12 000 g/mol) in DMF under Ar, followed by deprotection of the Z group. GPC measurement of PEG-*b*-PLL exhibited single sharp peak at Mw of 16,600 and Mn of 16,300 based on PEG standards. From the ^1H NMR measurement in D_2O, the polymerization degree of the PLL segment was determined to be 39.

2.3. Synthesis of dendrimer phthalocyanine

Dendrimer phthalocyanine (DPcZn) was prepared from dimethyl-5-hydroxyisophthalate and 4-nitrophthalonitrile according to the literature method (Scheme 1) [15]. Briefly, the hydroxy group of dimethyl-5-hydroxyisophthalate (**1**) was protected with a tert-butyldiphenylsilyl chloride to obtain 3-*tert*-butyldiphenylsilyloxy-dimethylisophthalate (**2**), and then the methyl ester groups were reduced to obtain 3-*tert*-butyldiphenylsilyloxy-5-hydroxymethyl benzyl alcohol (**3**), which was reacted with **1** using Mitsunobu's coupling reaction to obtain a silyl-protected G1 dendron (**4**). G1 dendron with phenol core (**5**) was obtained from **4** by deprotection reaction using tetrabutylammonium fluoride (TBAF). A silyl-protected G2 dendron (**6**) was synthesized from **5** by Mitsunobu's coupling reaction, and then deprotected to obtain G2 dendron with phenol core (**7**). The alkali mediated coupling reaction of **6** with 4-nitrophthalonitrile gave phthalonitrile-cored G2 dendron (**8**). A mixture of **8** and Zn $(OAc)_2$ in *n*-pentanol was heated at 90 °C, and then a few drops of 1,8-diazabicyclo[5,4,0]undec-7-ene (DBU) were added. The mixture was refluxed with stirring overnight. The reaction mixture was chromatographed with silica gel to obtain DPcZn.

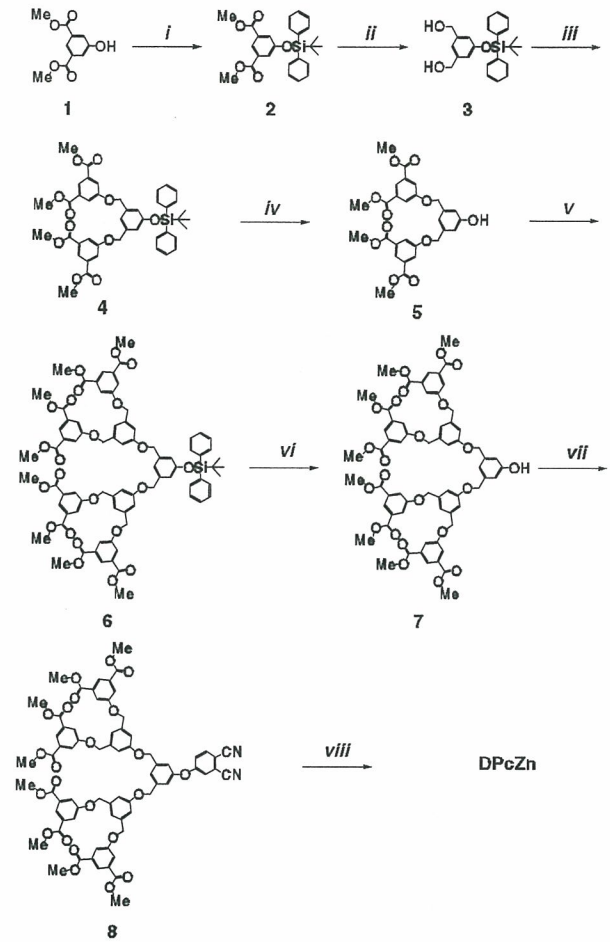

Scheme 1. Synthesis of phthalocyanine dendrimer. Reagents and conditions; (i) *tert*-butyldiphenylsilylchloride, imidazole, in DMF at 0 °C for 12 h; (ii) $LiAlH_4$ in THF at 0 °C for 12 h; (iii) **1**, diethylazodicarboxylate (DEAD), PPh3 in THF at 0 °C 12 h; (iv) tetrabutylammoniumfluoride (TBAF) in THF at 0 °C for 1 h; (v) **1**, DEAD, PPh3 in THF at 0 °C 12 h; (vi) TBAF in THF at 0 °C for 1 h; (vii) K_2CO_3, 4-nitrophthalonitrile, 18-crown in DMF at 60 °C for 12 h; (viii) Zn $(OAc)_2$, DBU in Pentanol reflux for 24 h.

2: yield 95%,^{1}H NMR δ 8.18 (m, 1H, Ar–*H* in phthalate), 7.70 (m, 4H, *o-H* in C_6H_5), 7.57 (m, 2H, Ar–*H* in phthalate), 7.40 (m, 6H, *m,p-H* in C_6H_5), 3.86 (s, 6H, $-OCH_3$), 1.13 (s, 9H, $-C(CH_3)_3$). **3**: yield 89%, ^{1}H NMR δ 7.64 (m, 4H, *o-H* in C_6H_5), 7.32 (m, 6H, *m,p-H* in C_6H_5), 6.80 (m, 1H, Ar–*H* in C_6H_3), 6.58 (m, 2H, Ar–*H* in C_6H_3), 4.41 (s, 4H, $-CH_2-$), 1.03 (s, 9H, $-C(CH_3)_3$). **4**: yield 64%, ^{1}H NMR δ 8.27 (s, 2H, Ar–*H* in outer C_6H_3), 7.73 (s, 4H, Ar–*H* in outer C_6H_3), 7.69 (m, 4H, *o-H* in C_6H_5), 7.40 (m, 6H, *m,p-H* in C_6H_5), 7.02 (s, 1H, Ar–*H* in inner C_6H_3), 6.58 (s, 2H, Ar–*H* in inner C_6H_3), 4.97 (s, 4H, $-CH_2-$), 3.94 (s, 12H, $-CH_3$), 1.01 (s, 9H, $-C(CH_3)_3$). **5**: yield 90%, ^{1}H NMR δ 8.27 (s, 2H, Ar–*H* in outer C_6H_3), 7.80 (d, 4H, Ar–*H* in outer C_6H_3), 7.05 (s, 1H, Ar–*H* in inner C_6H_3), 6.92 (s, 2H, Ar–*H* in inner C_6H_3), 6.13 (s, 1H, –O*H*), 5.08 (s, 4H, $-CH_2-$), 3.94 (s, 12H, $-CH_3$). **6**: yield 79%, ^{1}H NMR δ 8.26 (s, 4H, Ar–*H* in outer C_6H_3), 7.79 (s, 8H, Ar–*H* in outer C_6H_3), 7.69 (m, 4H, *o-H* in $-C_6H_5$), 7.35 (m, 6H, *m,p-H* in $-C_6H_5$), 7.04 (s, 2H, Ar–*H* in inner C_6H_3), 6.98 (s, 1H, Ar–*H* in inner C_6H_3), 6.94 (s, 4H, Ar–*H* in mid C_6H_3), 6.81 (s, 2H, Ar–*H* in mid C_6H_3) 5.10 (s, 8H, outer $-CH_2-$), 5.00 (s, 4H, inner $-CH_2-$), 3.93 (s, 24H, $-CH_3$), 1.08 (s, 9H, $-C(CH_3)_3$). **7**: yield 91%, ^{1}H NMR δ 8.27 (s, 4H, Ar–*H* in outer C_6H_3), 7.79 (s, 8H, Ar–*H* in outer C_6H_3), 7.36 (s, 2H, Ar–*H* in inner C_6H_3), 7.08 (s, 1H, Ar–*H* in inner C_6H_3), 7.01 (s, 4H, Ar–*H* in mid C_6H_3), 6.87 (s, 2H, Ar–*H* in mid C_6H_3), 6.37 (s, 1H, –O*H*), 5.11 (s, 8H, outer $-CH_2-$), 5.09 (s, 4H, inner $-CH_2-$) 3.93 (s, 24H, $-CH_3$). **8**: yield 90%, ^{1}H NMR δ 8.28 (s, 4H, Ar–*H* in outer C_6H_3), 7.80 (s, 8H, Ar–*H* in outer C_6H_3), 7.68 (d, 1H, Ar–*H* in phthalonitrile), 7.45 (s 1H, Ar–*H* in inner C_6H_3) 7.28–7.23 (m, 2H, Ar–*H* in phthalonitrile), 7.15 (s, 2H, Ar–*H* in inner C_6H_3), 7.14 (s, 2H, Ar–*H* in mid C_6H_3), 7.04 (s, 4H, Ar–*H* in mid C_6H_3), 5.16 (s, 4H, outer $-CH_2-$), 5.13 (s, 8H, inner $-CH_2-$) 3.93 (s, 24H, $-CH_3$). DPcZn: yield 32%, ^{1}H NMR δ 9.22–8.88 (m, 8H, Ar–*H*), 8.2–7.7 (m, 28H, Ar–*H*), 7.6–6.9 (m, 60H, Ar–*H*), 5.2–4.9 (m, 48H, $ArOCH_2-$), 4.2–4.0 (m, 64H, $-CO_2CH_2-$), 1.7–1.1 (m, 256H, $-CH_2-$), 0.9–0.7 (m, 96H, $-CH_3$), MALDI-TOF-MS for $C_{416}H_{496}N_8O_{92}Zn$ *m/z*: calcd.: 7139 [M^+]; found 7150.

2.4. Preparation of polyion complex micelle

Polyion complex micelles were made from charged DPcZn with PEG-*b*-PLL. In a typical procedure, the PEG-*b*-PLL was dissolved in an aqueous NaH_2PO_4 solution and added to an aqueous solution of DPcZn in Na_2HPO_4 to give a solution containing polyion complex micelles. The ratio of positive charge to negative charge was fixed at 1:1.

2.5. Measurements

The DLS measurements were performed using a Photal dynamic laser scattering DLS-7000 spectrometer (Otsuka Electronics Co., Ltd., Osaka, Japan) equipped with GLG3050 488 nm Ar laser (NEC Co., Ltd., Japan) and/or Zetasizer Nano ZS-90 (Malvern Co., Ltd., USA) with 532 nm laser irradiation. The UV–Vis and fluorescence spectra were measured using a V-550 spectrophotometer (JASCO, Tokyo, Japan) and Type 850 spectrofluorometer (Hitachi, Tokyo, Japan), respectively. MALDI-TOF-MS was performed on a Bruker model Protein TOF mass spectrometer with dithranol as the matrix. ^{1}H NMR spectroscopy was performed in $CDCl_3$ or D_2O on a JEOL GSX-270 spectrometer operating at 270 MHz. GPC was performed with TOSOH HLC-8220 equipped with TSK-gel G4000HHR and G3000HHR column (eluent: DMF+10 mM LiCl, temperature: 40 °C, detector: RI).

2.6. Oxygen consuming measurement

The oxygen consumption amount was measured using a Clark-type oxygen microelectrode with a tip diameter of 200 μm (PO_2-100DW, Eikou Kagaku Co., Ltd., Tokyo, Japan). The microelectrode was inserted into the PBS, which contained 3.13 μM of DPcZn or DPcZn/m and 10% FBS as a singlet oxygen acceptor, so that the tip was 100 μm above the bottom of the solution. Semiconductor laser light (660 nm; FWHM 6 nm, 25 mW/cm^2) was used for light irradiation. The solution was static and exposed to the atmosphere. Before each measurement, the system was calibrated in saline bubbled with air, in which the partial oxygen pressure was assumed to be 150 mm Hg.

2.7. Cell culture

HeLa cells were used in the cell culture studies. In the cytotoxicity assay, different concentration of DPcZn or DPcZn/m in Dulbecco's modified Eagle's medium (DMEM+10% FBS) were added to cells in 96-wll culture plates (n=4). After a 24 h incubation at 37 °C, the photosensitizers were removed, and then plates were photoirradiated for 15–60 min with broad-band visible light using a halogen lamp (150 W) equipped with a filter passing light of 400–700 nm (fluence energy; 27–107 kJ/m^2). The viability of the cells was evaluated using mitochondrial respiration via the 3-(4,5-dimethyl thiazole-2-yl)-2,5-diphenyltetrazolium bromide cleavage assay (MTT assay) following incubation for 48 h after photoirradiation or removing the photosensitizers by washing in the case of the dark toxicity investigation.

2.8. Cellular uptake amount

After incubation of HeLa cells with 10 μM of DPcZn or DPcZn/m for 24 h in 60-mm dishes, the cells were washed three times with PBS, and then dissolved in 20% SDS solutions for 24 h to give a homogenous solution. As a control experiment, HeLa cells were incubated without DPcZn or DPcZn/m addition and then dissolved in 20% SDS solutions include fixed amount of DPcZn or DPcZn/m. The homogeneous solution thus obtained was put into a quartz cell to measure fluorescence. Before measuring samples, it was confirmed that DPcZn or DPcZn/m has comparable intensity of fluorescence in the 20% SDS solution. Quantitative analysis of uptake amount of DPcZn and DPcZn/m by HeLa cells was performed on a fluorescence spectrophotometer (Type 850, Hitachi, Tokyo, Japan). The excitation wavelength was 630 nm, and the emission wavelength was measured from 650 to 900 nm. The number of HeLa cells was 60,000.

3. Results and discussion

3.1. Synthesis of dendrimer phthalocyanine and preparation of polyion complex micelle

The synthesis of the ionic dendrimer phthalocyanine was accomplished by the method of Ng's group [15]. The second generation of dendritic phenol was reacted with 4-nitrophthalonitrile by an alkali-mediated coupling reaction to obtain the corresponding dendritic phthalonitrile, which was then treated with $Zn(OAc)_2$ and DBU in *n*-pentanol to give dendrimer phthalocyanine. Each step of synthesis was characterized by MALDI-TOF-MS and ^1H NMR measurement, and reaction yields were almost comparable to the literature. The dendrimer phthalocyanine thus obtained was treated with a THF/H_2O mixture solution of NaOH to obtain ionic dendrimer phthalocyanine (DPcZn; Fig. 1). DPcZn exhibited significantly high solubility at various pHs of the aqueous medium (over pH 4.3).

A cationic block copolymer (poly(ethyleneglycol)-*block*-poly-L-lysine: PEG-*b*-PLL; Fig. 1) was synthesized by the polymerization of the *N*-carboxy anhydride of N^{ε}-Z-L-lysine, initiated by ω-aminated poly(ethyleneglycol) (CH_3O-PEG-NH_2:12,000 g/mol) in DMF, followed by deprotection of the Z group according to a previously reported method [17]. The degree of polymerization was determined to be 39, which was confirmed by ^1H NMR. GPC measurement exhibited single sharp peak and relatively small molecular weight value compare to ^1H NMR result because of the interaction between PLL segment and GPC column.

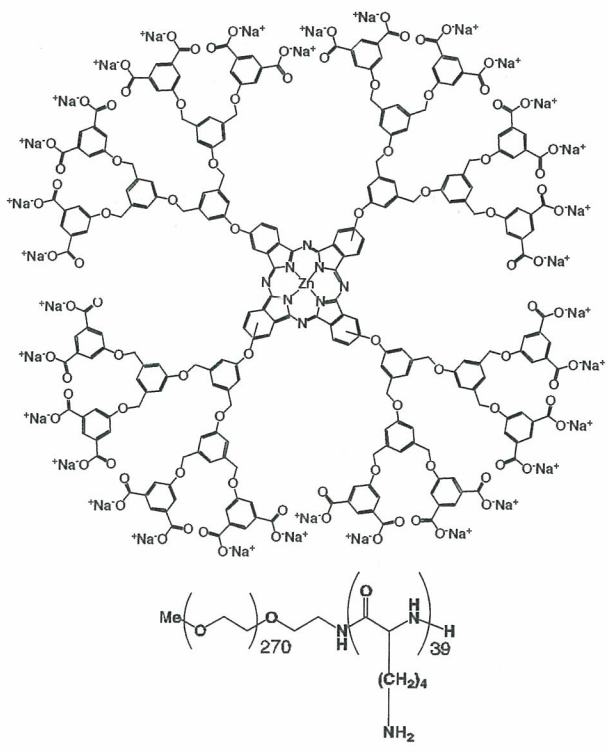

Fig. 1. Structures of DPcZn and PEG-*b*-PLL.

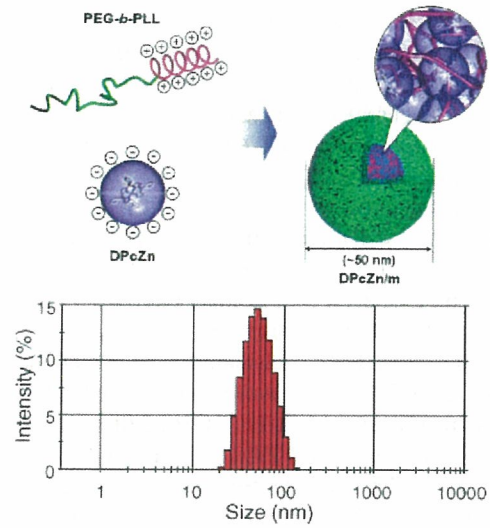

Fig. 2. Formation and DLS histogram analysis of polyion complex micelle (DPcZn/m).

Polyion complex micelles were prepared from negatively charged DPcZn with oppositely charged PEG-*b*-PLL. In a typical procedure, the PEG-*b*-PLL (14.2 mg) was dissolved in an aqueous NaH_2PO_4 (10 mM, 6.15 mL) and added to a solution of DPcZn (5 mg) in aqueous Na_2HPO_4 (10 mM, 13.85 mL) to give a solution containing polyion complex micelles encapsulating ionic DPcZn (Fig. 2). The ratio of positive charge to negative charge was fixed at 1:1. After mixing the two solutions, the pH of the solution becomes 7.3 (10 mM PBS). The resulting micelle has a diameter of ca. 50 nm with a narrow size distribution (unimodal, $\mu^2/\Gamma^2=0.12$), determined by a dynamic light scattering measurement (Zetasizer Nano ZS-90, Malvern Co., Ltd., USA) (Fig. 2). Furthermore, the diffusion coefficient of the resulting micelle was independent of the detection angle of the DLS measurement, suggesting that the polyion complex micelle of DPcZn with PEG-*b*-PLL is a narrowly dispersed spherical assembly.

3.2. Electronic absorption of dendrimer and micelle

Electronic absorption spectra of the dendrimer and micelle were measured (Fig. 3). DPcZn exhibits B band absorption at

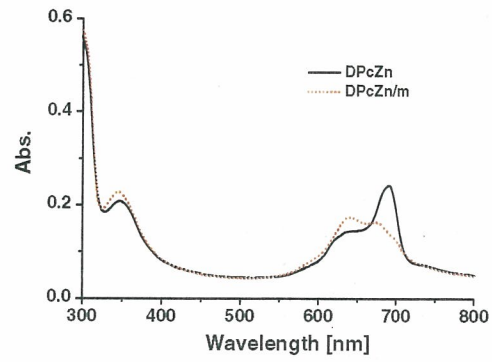

Fig. 3. Electronic absorption of DPcZn (15.3 μM) and DPcZn/m (15.3 μM) in 10 mM PBS.

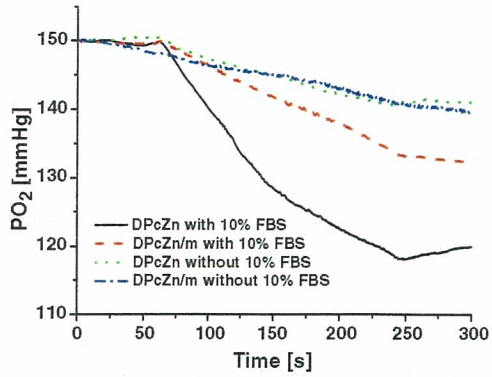

Fig. 4. Experimental setup for the measurement of oxygen consumption and the results obtained.

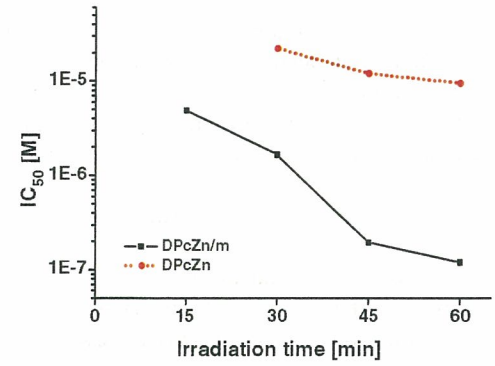

Fig. 6. Photoirradiation-time-dependent IC50 changes of DPcZn/m and DPcZn against HeLa Cells.

350 nm and strong Q band absorption at 685 nm, indicating successful dispersion as a monomeric species in the aqueous solution [16]. According to the formation of the polyion complex micelle, the absorption maximum of Q band absorption was slightly changed to 630 nm, indicating the possibility of slight aggregate formation of the core phthalocyanine units. Also, fluorescent intensity of DPcZn was drastically decreased by inclusion into the micelle (date not shown). The relatively small dendritic wedges may not perfectly prevent the aggregate formation of the phthalocyanine core units especially in the densely packed micellar core. Note that DPcZn (Mw=4901) is smaller than that of previously reported ionic dendrimer porphyrin (Mw=8029).

The absorption of light by tissue increases as the wavelength decreases and that the most efficient photosensitizers are those that have strong absorption bands between 600 and 800 nm. Therefore, although the relatively small dendritic wedges may not perfectly prevent collisional quenching, DPcZn has the potential for use as an effective photosensitizer in photodynamic therapy.

3.3. Oxygen consumption ability of the dendrimer phthalocyanine and micelle

The oxygen consumption amount was measured to evaluate ROS generation under photoirradiation [18]. Note that the DPcZn/m was sufficiently stable in the 10 mM PBS with 10% FBS, where the size and polydispersity of DPcZn/m in the 10 mM PBS with 10% FBS were almost comparable to those without FBS (data not shown). The oxygen partial pressure (PO_2) of DPcZn solution is significantly reduced by the irradiation of laser light (660 nm; FWHM 6 nm, 25 mW/cm^2) (Fig. 4). Although the consumption ability of DPcZn/m was lower than that of DPcZn, the PO_2 of DPcZn/m solution was also effectively reduced, indicating that either DPcZn or DPcZn/m can take part in the photochemical reaction to generate ROS. On the other hand, either DPcZn or DPcZn/m solution without 10%

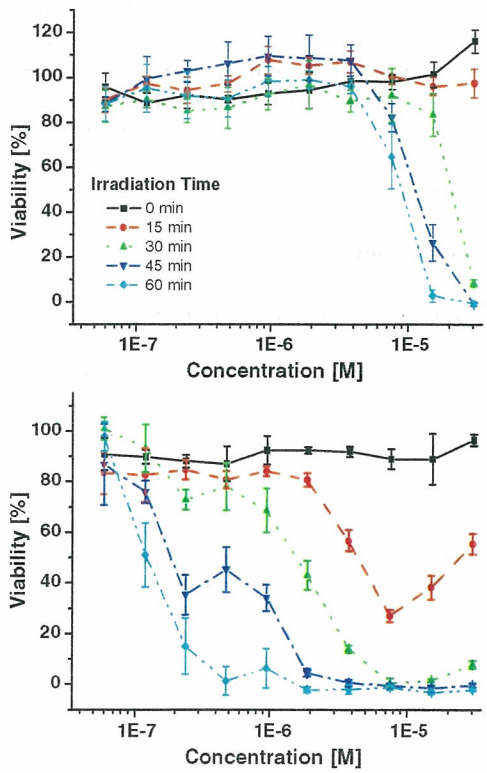

Fig. 5. Photocytotoxic profiles of DPcZn (top) and DPcZn/m (bottom) against HeLa cells.

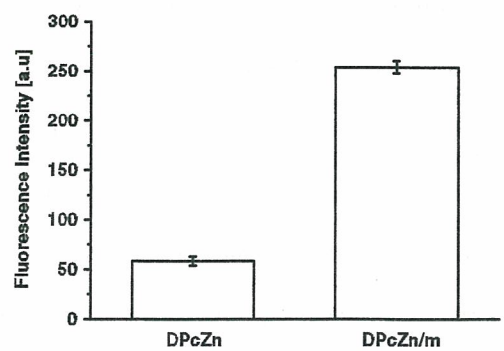

Fig. 7. Relative fluorescence intensities of uptaken DPcZn and DPcZn/m into HeLa cells. 10 μM of DPcZn or DPcZn/m was incubated with HeLa cells for 24 h. The excitation wavelength was 630 nm, and the fluorescence intensity was recorded from 650 to 900 nm.

FBS shows almost negligible change in the PO_2 upon the photoirradiation, indicating that the proteins in FBS act as sacrificial acceptors of ROS. In other words, if proteins do not exist in the medium, once generated, ROS promptly revert to oxygen molecules because of their short lifetimes.

3.4. Cytotoxicity of dendrimer phthalocyanine and micelle

The cytotoxicity of phthalocyanine dendrimer was assessed against HeLa cells (Fig. 5). The viability of cells upon photoirradiation was evaluated by MTT assay and determined to be a function of concentration and photoirradiation time with DPcZn and its micelle. DPcZn and DPcZn/m were incubated with the cells for 24 h and then fully washed with PBS to remove non-associated photosensitizers prior to photoirradiation. Under dark conditions, toxicities of DPcZn and DPcZn/m were negligible. However, either DPcZn or DPcZn/m exhibited photoinduced cytotoxicity upon the photoirradiation, where the cells were photoirradiated for 15–60 min with broad-band visible light using a halogen lamp (150 W) equipped with a filter passing light of 400–700 nm (fluence energy: 27–107 kJ/m^2). According to the exposure time increase, either DPcZn or DPcZn/m exhibited an increase in photocytotoxicity (Fig. 5). Very interestingly, the aspect of the photocytotoxicity increase is significantly different between DPcZn and DPcZn/m. As shown in Fig. 6, DPcZn exhibits a relatively small time-dependency, whereas DPcZn/m exhibits a remarkable change in the cell viability depending on the photoirradiation time. Typically at 60-min photoirradiation, DPcZn/m exhibited almost 100 times higher photocytotoxicity than free DPcZn. Although electronic absorption and oxygen consumption behaviours exhibited quenching signature, DPcZn/m have significantly high PDT efficacy compare to DPcZn alone. On the other hand, the cell viability exhibits abnormal increase with increase in the concentration of DPcZn/m at the 15-min light irradiation. There is various reasons can be considerable such as compositional change of micellar structure or microenvironment change around photosensitizers. To understand this phenomenon, we need further investigation.

In view of the negatively charged surface of mammalian cells, charge neutralization of DPcZn by formulation of micelle possibly improves the cellular uptake. In fact, DPcZn/m showed a 4 times higher cellular uptake compared to DPcZn alone when HeLa cells were incubated with 10 μM of DPcZn or DPcZn/m for 24 h (Fig. 7). Nevertheless, the enhancement of photocytotoxicity by the micelle formulation is much larger than the improvement in cellular uptake. Furthermore, this result is quite controversial to the quenching signature of DPcZn within the micellar core.

This phenomenon presumably suggests that the PEG shell layer of the DPcZn/m and micro environment around DPcZn may have a role in altering the intracellular mechanism of DPcZn to increase the photocytotoxicity. Also, in the case of DPcZn/m, a large amount of ROS can be generated at once within the micellar core. Therefore, the higher local concentration of ROS around the micelle may easily exceed the threshold of photodamage against typical cellular organelles.

The remarkably enhanced photocytotoxicity of the micellar system may be very advantageous point for practical applications. Because the most of photosensitizers have large π-conjugation domain and hydrophobic skeleton, photosensitizers easily form aggregates within the highly concentrated micellar core via π–π and hydrophobic interactions. The formation of aggregates result in the collisional quenching of the excitation state, photocytotoxicity will be impaired when the micellar structure occurs [19]. In contrast, because DPcZn shows less collisional quenching by micelle formation due to the large dendritic wedges, photocytotoxicity will be maintained, or even enhanced in the micelle form. The DPc-incorporated micelle is assumed to gradually dissociate into the constituent DPc and block copolymer in the body by dilution; therefore, eventually long-term phototoxicity due to non-specific uptake of photosensitizers in normal tissue may be avoidable after PDT using this micelle system [20]. Actually, our recent experiment showed that the dendritic photosensitizers have almost no skin toxicity under light irradiation compared to the clinically used photosensitizer formulation Photofrin® [21,22].

4. Conclusions

The first example of polyion complex micelle formation of DPcZn and its photodynamic efficacy were demonstrated. DPcZn/m exhibited long wavelength absorption around 650 nm, which is very advantageous for the treatment of deep lesions, because the long wavelength light is less absorbed by melanin dyes in skin tissue or heme proteins in blood. Furthermore, the micellar formulation may improve the longevity in blood circulation that achieves cumulative accumulation in the lesion with hyperpermeability, such as a macular degeneration [23], due to the enhanced permeation and retention (EPR) effect [24]. The in vivo PDT efficacy of DPcZn/m is now under investigation in our research group using disease models, such as cancer and macular degeneration.

Acknowledgement

This study was supported by Industrial Technology Research Grant Program in 2004 from New Energy and Industrial Technology Development Organization (NEDO) of Japan.

References

[1] R.K. Pandey, G. Zhang, in: K.M. Kadish, K.M. Smith, R. Guilard (Eds.), Porphyrin Handbook, vol. 6, Academic press, New York, 2000, pp. 157–230.
[2] I.J. Macdonald, T.J. Dougherty, Basic principles of photodynamic therapy, J. Porphyr. Phthalocyanines 5 (2) (2001) 105–129.
[3] Y. Takeuchi, K. Ichikawa, S. Yonezawa, K. Kurohane, T. Koishi, M. Nango, Y. Namba, N. Oku, Intracellular target for photosensitization in cancer antiangiogenic photodynamic therapy mediated by polycation liposome, J. Control. Release 97 (2) (2004) 231–240.
[4] N. Merclin, T. Bramer, K. Edsman, Iontophoretic delivery of 5-aminolevulinic acid and its methyl ester using a carbopol gel as vehicle, J. Control. Release 98 (1) (2004) 57–65.
[5] Y.N. Konan-Kouakou, R. Boch, R. Gurny, E. Allemann, In vitro and in vivo activities of verteporfin-loaded nanoparticles, J. Control. Release 103 (1) (2005) 83–91.

[6] N. Tomioka, D. Takasu, T. Takahashi, T. Aida, Electrostatic assembly of dendrimer electrolytes: negatively and positively charged dendrimer porphyrins, Angew. Chem., Int. Ed. Engl. 37 (11) (1998) 1531–1534.
[7] N. Nishiyama, H.R. Stapert, G.D. Zhang, D. Takasu, D.L. Jiang, T. Nagano, T. Aida, K. Kataoka, Light-harvesting ionic dendrimer porphyrins as new photosensitizers for photodynamic therapy, Bioconjug. Chem. 14 (1) (2003) 58–66.
[8] H.R. Stapert, N. Nishiyama, D.L. Jiang, T. Aida, K. Kataoka, Polyion complex micelles encapsulating light-harvesting ionic dendrimer zinc porphyrins, Langmuir 16 (21) (2000) 8182–8188.
[9] W.-D. Jang, N. Nishiyama, G.-D. Zhang, A. Harada, D.-L. Jiang, S. Kawauci, Y. Morimoto, M. Kikuchi, H. Koyama, T. Aida, K. Kataoka, Supramolecular nanocarrier of anionic dendrimer porphyrins with cationic block copolymers modified with polyethylene glycol to enhance intracellular photodynamic efficacy, Angew. Chem., Int. Ed. Engl. 44 (3) (2005) 419–423.
[10] T. Sato, D.-L. Jiang, T. Aida, A blue-luminescent dendritic rod: poly (phenyleneethynylene) within a light-harvesting dendritic envelope, J. Am. Chem. Soc. 121 (45) (1999) 10658–10659.
[11] S.A. Gerhardt, J.W. Lewis, D.S. Kliger, J.Z. Zhang, U. Simonis, Effect of micelles on oxygen-quenching processes of triplet-state para-substituted tetraphenylporphyrin photosensitizers, J. Phys. Chem., A 107 (15) (2003) 2763–2767.
[12] Y. Kakizawa, K. Kataoka, Block copolymer micelles for delivery of gene and related compounds, Adv. Drug Deliv. Rev. 54 (2) (2002) 203–222.
[13] E.A. Lukyanets, Phthalocyanines as photosensitizers in the photodynamic therapy of cancer, J. Porphyr. Phthalocyanines 3 (6–7) (1999) 424–432.
[14] P.-C. Lo, J.-D. Huang, D.Y.Y. Cheng, E.Y.M. Chan, W.-P. Fong, W.-H. Ko, D.K.P. Ng, New amphiphilic silicon(IV) phthalocyanines as efficient photosensitizers for photodynamic therapy: synthesis, photophysical properties, and in vitro photodynamic activities, Chem. Eur. J. 10 (19) (2004) 4831–4838.
[15] A.C.H. Ng, X. Li, D.K.P. Ng, Synthesis and photophysical properties of nonaggregated phthalocyanines bearing dendritic substituents, Macromolecules 32 (16) (1999) 5292.
[16] Z. Sheng, X. Ye, Z. Zheng, S. Yu, D.K.P. Ng, T. Ngai, C. Wu, Transient absorption and fluorescence studies of disstacking phthalocyanine by poly (ethylene oxide), Macromolecules 35 (9) (2002) 3681–3685.
[17] A. Harada, K. Kataoka, Formation of polyion complex micelles in an aqueous milieu from a pair of oppositely-charged block copolymers with poly(ethylene glycol) segments, Macromolecules 28 (15) (1995) 5294–5299.
[18] S. Kawauchi, S. Sato, Y. Morimoto, M. Kikuchi, Correlation between oxygen consumption and photobleaching during in vitro photodynamic treatment with ATX-S10(Na(II) using pulsed light excitation: Dependence of pulse repetition rate and irradiation time, Photochem. Photobiol. 80 (2004) 216–223.
[19] W. Spiller, H. Kliesch, D. Wöhrle, S. Hackbarth, B. Röder, G. Schnurpfeil, Singlet oxygen quantum yields of different photosensitizers in polar solvents and micellar solutions, J. Porphyr. Phthalocyanines 2 (2) (1998) 145–158.
[20] S.B. Brown, E.A. Brown, I. Walker, The present and future role of photodynamic therapy in cancer treatment, Lancet Oncol. 5 (8) (2004) 497–508.
[21] Y. Nakagishi, Y. Morimoto, S. Kawauchi, W.-D. Jang, N. Nishiyama, Y. Ozeki, K. Kataoka, M. Kikuchi, Photodynamic therapy combined with drug delivery system using a macromolecular polymeric micelle, Abstracts of 96th Annual Meeting 2005-American Association for Cancer Research, Anahim, USA, April 16-20, 2005.
[22] R. Ideta, F. Tasaka, W.-D. Jang, N. Nishiyama, G.-D. Zhang, Aou. Harada, Y. Yanagi, Y. Tamaki, T. Aida, K. Kataoka, Nanotechnology-based photodynamic therapy for neovascular disease using a supramolecular nanocarrier loaded with a dendritic photosensitizer, Nano Lett. 5 (2005) 2426–2431.
[23] D.N. Zacks, E. Ezra, Y. Terada, N. Michaud, E. Connolly, E.S. Gragpidas, J.W. Miller, Verteporfin photodynamic therapy in the rat model of choroidal neovascularization: angiographic and histologic characterization, Invest. Ophthalmol. Vis. Sci. 43 (2002) 2384–2391.
[24] H. Maeda, J. Wu, T. Sawa, Y. Matsumura, K. Hori, Tumor vascular permeability and the EPR effect in macromolecular therapeutics: a review, J. Control. Release 65 (1–2) (2000) 271–284.

GENE DELIVERY

ELSEVIER

Available online at www.sciencedirect.com
ScienceDirect
Journal of Controlled Release 115 (2006) 208–215

journal of controlled release
www.elsevier.com/locate/jconrel

PEGylated gene nanocarriers based on block catiomers bearing ethylenediamine repeating units directed to remarkable enhancement of photochemical transfection

Arnida [a], Nobuhiro Nishiyama [b,c,*], Naoki Kanayama [a,d], Woo-Dong Jang [e], Yuichi Yamasaki [a,c,d], Kazunori Kataoka [a,b,c,d,*]

[a] *Department of Materials Engineering, Graduate School of Engineering, The University of Tokyo, 7-3-1 Hongo, Bunkyo-ku, Tokyo 113-8656, Japan*
[b] *Center for Disease Biology and Integrative Medicine, Graduate School of Medicine, The University of Tokyo, 7-3-1 Hongo, Bunkyo-ku, Tokyo 113-0033, Japan*
[c] *Center for NanoBio Integration, The University of Tokyo, 7-3-1 Hongo, Bunkyo-ku, Tokyo 113-8656, Japan*
[d] *Core Research for Evolutional Science and Technology (CREST) from the Japan Science and Technology Agency (JST), Japan*
[e] *Department of Chemisty, College of Science, Yonsei University, 134 Sinchondong, Seodaemun-gu, Seoul 120-749, Korea*

Received 26 May 2006; accepted 17 July 2006
Available online 20 July 2006

Abstract

The therapeutic usefulness of macromolecular drugs such as plasmid DNA is often limited by the inefficient transfer of macromolecules to the cytosol. Photochemical internalization (PCI) technology, in which the endosomal escape of DNA or its complex is assisted by co-incubated photosensitizers that photodamage endosome membrane, offers a solution for this problem. A series of poly(ethylene glycol) (PEG)-based block polycatiomers with increasing number of ethylenediamine repeating unit at side chain of polycatiomers were complexed with pDNA to form the PEGylated polyplexes as a biocompatible gene carrier. Dendrimeric phthalocyanine (DPc)-incorporated micelle was used to assist the gene transfer of these polyplexes in a light-inducible manner. As a result, the light-inducible transfection activity was significantly enhanced as the number of amino group at the side chain of PEG-*b*-polycatiomer increased. The polyplex from PEG-*b*-polycatiomer having the longest ethylenediamine structure achieved approximately 1000-fold enhancement of transfection upon photoirradiation. This result supports the underlying hypothesis that photochemical transfection and proton sponge effect of polycations can work synergistically to enhance the transfection efficiency. With careful balance between photochemical transfection enhancement and cytotoxicity, PEG-*b*-polycatiomers used in this study might be a potential candidate for *in vivo* PCI-mediated gene transfer.

Keywords: Gene delivery; Polyplex; Polymeric micelle; Photochemical internalization; Photosensitizer

1. Introduction

Gene therapy is a promising approach to conquer intractable diseases for which there is little hope of finding conventional cure. But it still poses several hurdles that need to be overcome before it could enter a clinical phase. Gene therapy mostly depends on the development of the methods for efficient and specific delivery of the gene into the target cells [1–3]. Using viruses as a vector is limited by the safety factor and difficulties in production. By contrast, synthetic gene carriers are versatile and safe, however, its transfection ability might be substantially lower than viral vector [4]. A great deal of challenges in developing non-viral vectors, especially polycatiomer based gene carriers are ongoing in the world.

In non-viral or polycatiomer-mediated gene delivery, endosomal membrane could be a major biological barrier that should be overcome to deliver DNA or its complex to cytosol. In this regard, polyethylenimine (PEI) has been successfully used for the transfection of various types of cells. The early escape of the PEI/DNA complexes from the endosome, arising from "proton

* Corresponding authors. Kataoka is to be contacted at Department of Materials Engineering, Graduate School of Engineering, The University of Tokyo, 7-3-1 Hongo, Bunkyo-ku, Tokyo 113-8656, Japan. Nishiyama, Center for Disease Biology and Integrative Medicine, Graduate School of Medicine, The University of Tokyo, 7-3-1 Hongo, Bunkyo-ku, Tokyo 113-0033, Japan. Tel.: +81 3 5841 7138; fax: +81 3 5841 7139.
E-mail addresses: nishiyama@bmw.t.u-tokyo.ac.jp (N. Nishiyama), kataoka@bmw.t.u-tokyo.ac.jp (K. Kataoka).

0168-3659/$ - see front matter © 2006 Elsevier B.V. All rights reserved.
doi:10.1016/j.jconrel.2006.07.014

sponge effect" was postulated to be the cause of high transfection efficiency [5–7]. However, the polyplexes based on PEI might usually contain an excess of free polymer that is not complexed with DNA. Ultrafiltration or size exclusion chromatography (SEC) can remove free PEI from the polyplexes; however, the purified polyplexes displayed lower transfection efficiency at low DNA concentration [8].

On the other hand, Berg et al. have introduced a novel technology called "photochemical internalization (PCI)", which allows the endosomal escape of the polyplexes in a light-inducible manner. This technology is based upon light activation of photosensitizer specifically locating at the membrane of endocytic vesicles and photochemically disrupting the membrane to release the content from endosome to cytoplasm [9–12]. This method enables the site-specific gene expression in a light-sensitive manner. Indeed, this strategy allowed the light-induced transfection; however, the enhancement of gene expression was accompanied by the photocytotoxicity [11]. The photodamage to sensitive organelles other than endosomal membrane, e.g., the plasma and mitochondrial membranes might be responsible for such photocytotoxicity [13]. Hence, increasing the selectivity of the photodamage to the endosome/lysosome is assumed to lead to the photochemical enhancement of transfection with reduced cytotoxicity. Recently, a ternary complex enveloped with anionic dendrimer phthalocyanine photosensitizer has been developed to achieve the PCI-mediated gene delivery [14]. The ternary complexes showed an expanded range of safe light dose where the photochemical enhancement of the transfection was achieved with a minimal photocytotoxicity, resulting in the success of this system for PCI-mediated gene delivery *in vivo* by local injection [14]. However, this ternary complex system is unlikely to be used for the systemic delivery due to its highly negative charges, which might be recognizable by the scavenger receptor [15]. Hence, it might be required to develop the light-responsive gene carrier applicable for the systemic delivery.

Alternatively, we have developed a biocompatible gene carrier, polyplex micelle based on the micellar assembly of the polyion complex (PIC) with block copolymer consisting poly (ethylene glycol) (PEG) and polycation segments. Their excellent properties for *in vitro* and *in vivo* application have been confirmed such as increased nuclease resistance and high stability under physiological conditions [16,17]. However, the polyplex micelles formed from PEG-*block*-poly(L-lysine) (PEG-*b*-PLL) copolymers possess significantly low transfection ability, which might be due to their inefficient transport from the endosome/lysosome to the cytosol [18]. In this regard, the feasibility of the use of the combination of polymeric micelles incorporating pDNA and dendrimer phthalocyanine (DPc) photosensitizer for PCI-mediated gene delivery has been carried out using PEG-*b*-PLL as carriers. The usefulness of this system for transfection enhancement *in vitro* was successfully demonstrated [19]. This system might be useful for *in vivo* application after systemic delivery. The schematic illustration of this strategy is shown in Fig. 1.

Motivated by this success, we tried to find another vector for pDNA other than PEG-*b*-PLL that might show higher photochemical transfection efficiency. In addition, we also intend to elucidate the structure–photochemical transfection efficiency

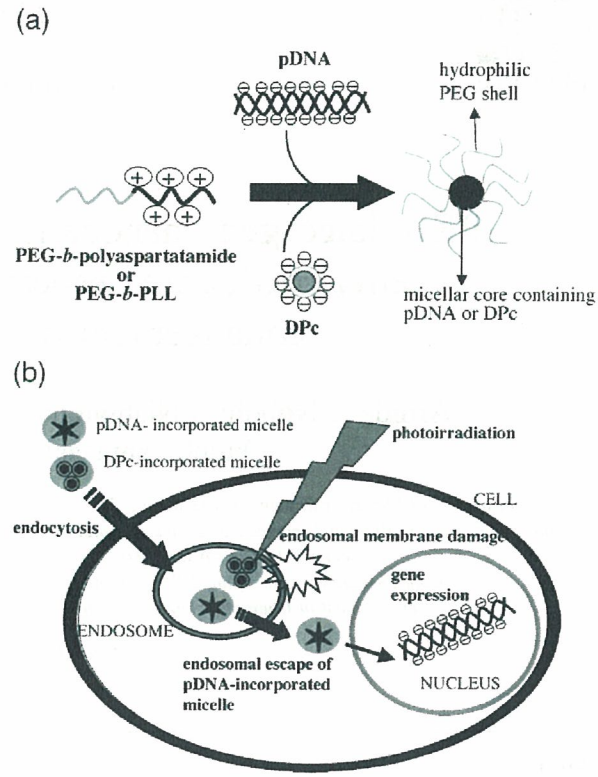

Fig. 1. Schematic illustration of (a) formation of pDNA- and DPc-incorporated micelles through electrostatic interaction between PEG-polycatiomer and pDNA or negatively charged DPc; (b) intracellular trafficking of the pDNA- and DPc-incorporated micelles in the PCI-mediated transfection. Both polymeric micelles are assumed to be taken up by the cell through the endocytic pathway. The localization of the DPc-incorporated micelles in the endosome may allow the selective photodamaging to the endosomal membrane upon photoirradiation, thereby inducing the cytoplasmic delivery of the pDNA-incorporated micelles.

relationship. In the present study, a series of PEG-*b*-polycatiomers bearing a different number of ethylenediamine repeating units at the side chain were used. Recently, we have successfully synthesized PEG-*b*-polyaspartatamide copolymers carrying the ethylenediamine unit at the side chain, which showed an appreciable buffering capacity under endosomal acidic conditions [20]. We hypothesize that the use of buffering polycations may assist the photochemical disruption of the endosomal membrane, thereby accelerating the cytoplasmic delivery of the polyplex micelles upon photoirradiation. The combination of polyplex micelles and DPc micelles was used for PCI-mediated gene transfer in this study.

2. Experimental section

2.1. Materials

N-[*tert*-Butoxycarbonyl (*Z*)]-L-lysine and bis(trichloromethyl)carbonate (triphosgene), for the synthesis of PEG-*b*-PLL diblock catiomers, were purchased from Sigma Aldrich Co., Inc. (St. Louis, MO) and Tokyo Kasei Co., Ltd. (Tokyo, Japan), respectively. β-Benzyl-L-aspartate-*N*-carboxy anhydride (BLA-NCA) and α-methoxy-ω-aminopoly(ethylene glycol)